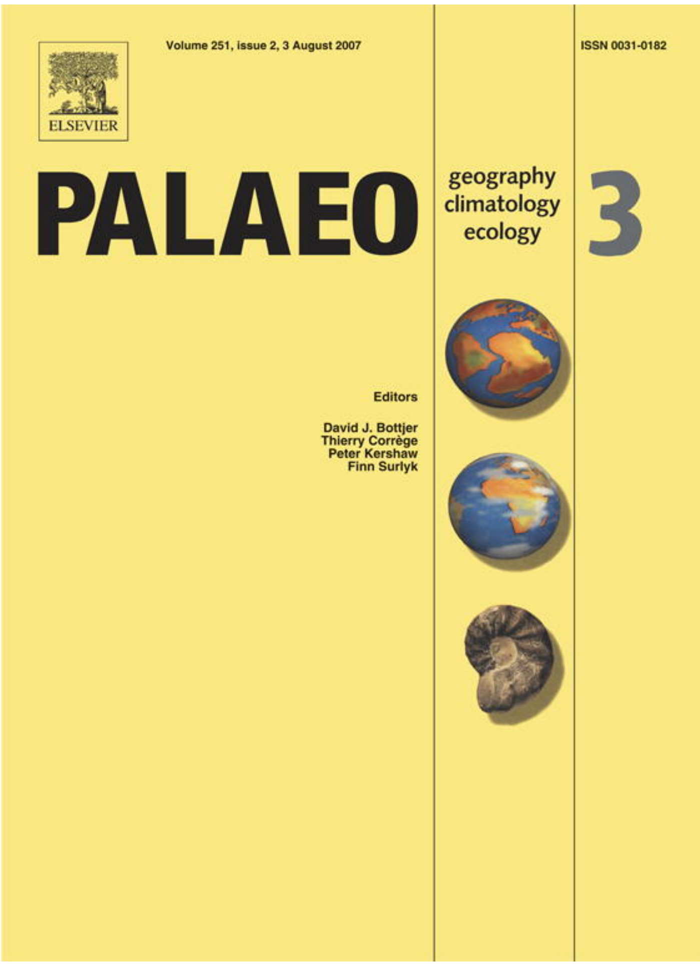
Volume 251, issue 2, 3 August 2007
ISSN 0031-0182
ELSEVIER
PALAEO
geography
climatology
ecology
3
Editors
David J. Bottjer
Thierry Corrège
Peter Kershaw
Finn Surlyk

Available online at www.sciencedirect.com
ScienceDirect
ELSEVIER
Palaeogeography, Palaeoclimatology, Palaeoecology 251 (2007) 300–320
PALAEO
www.elsevier.com/locate/palaeo

Geomorphology and chronology of Late Quaternary dune fields of western Argentina

Alfonsina Tripaldi [a], Steven L. Forman [b,*]

[a] *Department of Geology, University of Buenos Aries, Ciudad Universitaria, Buenos Aries, C1428EHA, Argentina*
[b] *Department of Earth and Environmental Sciences, University of Illinois at Chicago, Chicago, IL 60607, USA*

Received 14 September 2006; received in revised form 21 March 2007; accepted 5 April 2007

Abstract

Stabilized dune fields are common in western Argentina and potentially reflect drought variability in the Late Quaternary. This study focussed on deciphering geomorphic and stratigraphic record of three vegetated dune fields from east to west, San Luis, Médanos Negros and Médanos Grandes, with a mean annual precipitation from ∼700 to 91 mm. Optically stimulated luminescence single-aliquot regeneration protocols yield ages on eolian quartz grains, constraining depositional events. The San Luis dune field, the wettest area, exhibits evidence for repeated activation during the last glaciation, ca. 33–20 ka, generally coincident with regional loess deposition These dunes were locally reformed in the past 100 years which is apparently coincident with intensified agrarian use and drying in the late 19th and early 20th century. The two driest and western-most dune fields, Médanos Negros and Médanos Grandes, show reactivation at ca. 2.5 ka 0.9 and 0.5 ka; and ca. 4.3–4, 2.1 and 0.6–0.4 ka, respectively. Eolian depositional events at ca. 2.5–2.1 ka and 0.6–0.4 ka may be coeval for Médanos Grandes and Negros dune fields. Sustained drought conditions conducive for eolian activity is associated with warmer sea surface temperatures in the South Atlantic, a weakened South American Convergent Zone and a dispersed and southeasterly flow of tropical moisture from the Low Level Chaco Jet. This nascent analysis indicates drought variability beyond historic observations with potentially at least four dune reactivation events in the past ca. 4.5 ka.

Keywords: Dune fields; Eolian; Argentina; Climate variability

1. Introduction

Loess and eolian sand are common surficial deposits on the Pampas of Argentina (e.g. Iriondo and Kröhling, 1996; Kröhling, 1999a; Muhs and Zárate, 2001; Sayago et al., 2001; Zárate, 2003). These extensive eolian deposits (Fig. 1) are principally related to uplift and enhanced glaciation of the Andes since the Miocene, augmented in the Quaternary with volcanic ash input (Clapperton, 1993; Zárate, 2003). Large east flowing rivers emanating from the Andes with extensive flood plains are the principle source of Pleistocene eolian sediments (Zárate and Blasi, 1993; Zárate, 2003). Concomitant with loess deposition at least in the past ca. 70 ka was episodic deposition of eolian sand with the development of multiple ergs across the Pampas and is referred to as the “Pampean Sand Sea” (Iriondo and Kröhling, 1996; Iriondo, 1999; Kröhling, 1999a,b).

* Corresponding author.
E-mail addresses: alfo@gl.fcen.uba.ar (A. Tripaldi), slf@uic.edu (S.L. Forman).

0031-0182/$ - see front matter © 2007 Elsevier B.V. All rights reserved.
doi:10.1016/j.palaeo.2007.04.007

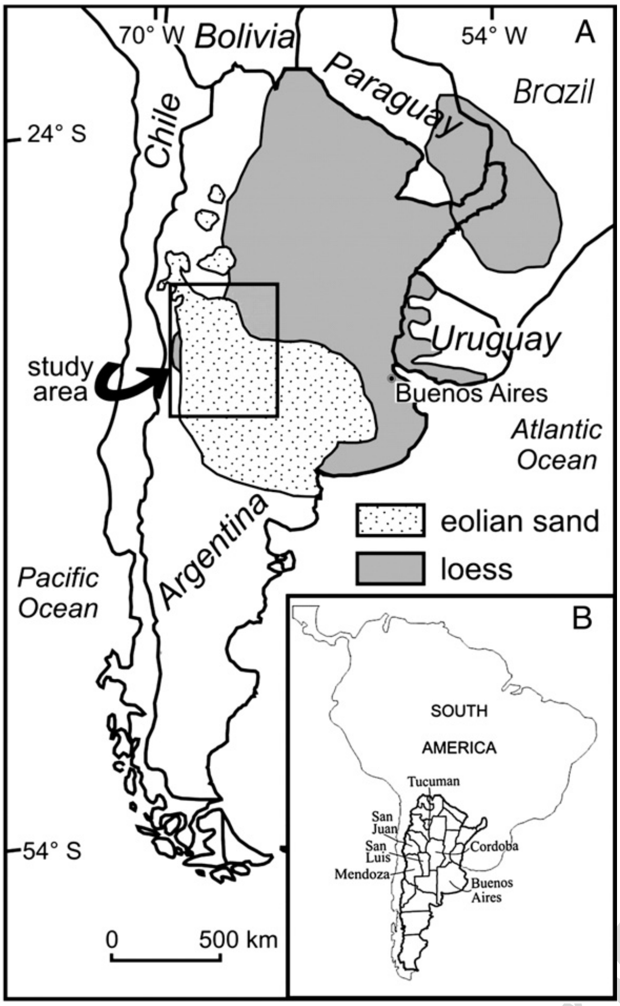

Fig. 1. (A) Argentina and mentioned provinces, (B) Distribution of eolian sand (dotted) and loess (shaded) in Argentina, Paraguay, Brazil and Uruguay (modified from Zárate, 2003).

Large ergs also occurs farther to the west in intermontane areas of the Sierras Pampeanas, Precordillera and the Andes (Fig. 2) (Tripaldi, 2002a,b; Tripaldi and Limarino, 2004).

The extent and depositional age of the sand seas is not well known. Thermoluminescence ages indicate that an extensive dune field formed in southern Sante Fe Province at ca. 70–65, 52–45 and 36–32 and 16 ka and is associated with colder and drier conditions during glacials (Krohling, 1999b). Discontinuous loess deposition ensued between ca. 14 and 8.5 ka and is associated with late glacial drying (Krohling, 1999b). Intervals of eolian deposition have also been recognized in central Argentina (Córdoba Province) durial glacial and potentially interglacial intervals ca. 100 ka and from 22 ka to the middle Holocene (Kemp et al., 2006). A pronounced eolian sand and loess depositional episode at ca. 36 to 8.5 ka was documented in Mar Chiquita, east central Córdoba Province (Kröhling and Iriondo, 1999). This cold and dry episode was interrupted by a wet period at ca. 15.5 to 16.5 ka ago. Lake level rose in Mar Chiquita ca. 8.5 to 3.0 ka, associated with generally mesic condition and landscape stability and pedogenesis (Kröhling and Iriondo, 1999). At other localities on the southern Pampas pollen analysis indicates that warm and humid conditions persisted sometime between 10.5 and 5.0 ka (Prieto, 1996), whereas the morphology of buried soils in northwestern Argentina indicate mesic conditions 8.5 and 6.4 ka (Alcalde and Kulemeyer, 1999).

Eolian activity renewed with pervasive drying in the late Holocene (ca. 3.5 to 1.4 ka). Regional drying may have commenced earlier indicated by discontinuous loess deposits that date between ca. 6 and 3 ka from Córdoba Province (Sanabria and Argüello, 1999). This drying may have been widespread as recognized in sedimentary records spanning the past 3 ka from Buenos Aries Province (Iriondo, 1990; Iriondo and García, 1993) and Sante Fe Province (Kröhling, 1999a,b). A number of pollen records from Mendoza Province show drying initiated by ca. 8 ka with peak drying associated with monte type vegetation at 6 to 4 ka (D'Antoni, 1983; García et al., 1999; Mancini et al., 2005). Aridity in the early to middle Holocene (ca. 9 to 4 ka) is well documented in lacustrine sedimentary records from the Bolivian and the northern Chilean Altiplano and northwestern Argentina (Markgraf, 1989; Villagrán and Varela, 1990; Martin et al., 1993; Grosjean et al., 1997; Sandweiss et al., 1999; Jenny et al., 2002). This drying may have been sufficiently severe to restrict habitation of southern Mendoza Province in western Argentina, reflected by the near disappearance of archaeologic sites between ca. 6 and 4 ka (Gil et al., 2005). A recent eolian event, sometime in the past 0.5 ka, is associated with the formation of dunes and deflation basins (Cioccale, 1999) and partial reactivation of dune forms; this event may be coeval with inferred Little Ice Age aridity on the western Pampas (Krohling, 1999b). Eolian sand is clearly ubiquitous in the western Pampas and adjacent intermontane valleys and may reflect significant climate variability in the Late Quaternary and Holocene as indicated by other proxy climatic records (e.g. Villalba, 1994; Villalba et al., 1998; Cioccale, 1999; Valero-Garcés et al., 2001; Piovano et al., 2004; Espizua, 2005); however, this dune field record has yet to be adequately deciphered.

The focus of this paper are three representative and vegetated dune fields from western Argentina, specifically from east to west, San Luis (SL), Médanos Negros (MN) and Médanos Grandes (MG) dune fields (Fig. 2),

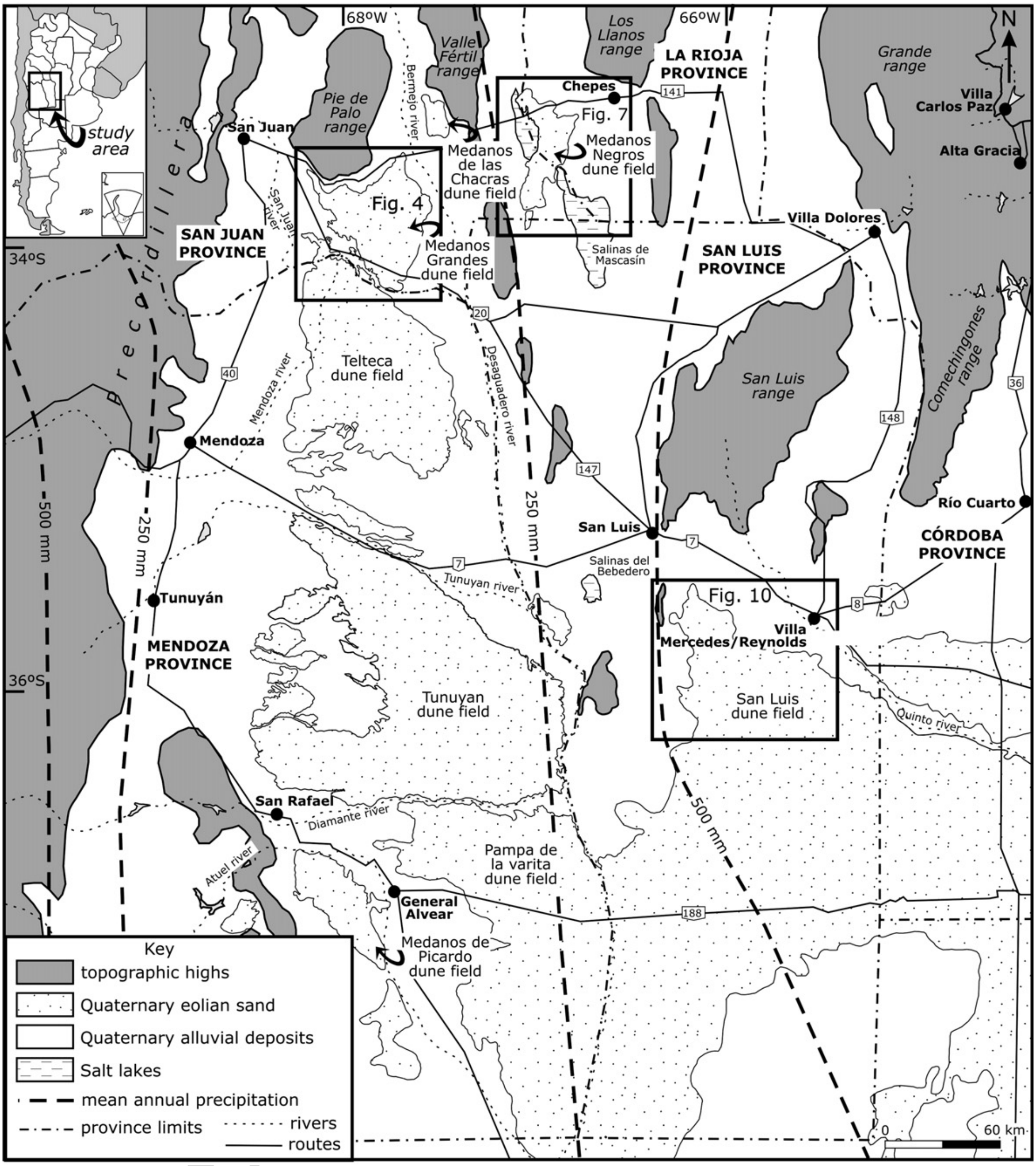

Fig. 2. Distribution of dune fields in relation to mountain ranges for central-western Argentina.

for which little is known about the Late Quaternary to Holocene depositional history. We provide a geomorphic assessment for each stabilized dune field and present the first stratigraphic records of eolian deposition with luminescence age control. This nascent environmental record yields a new context for understanding temporal and spatial variability in eolian processes and associated aridity in southern South America.

2. Climatologic context

The studied dune fields, San Luis, Médanos Negros and Médanos Grandes, lie on a precipitation gradient with mean annual values decreasing east to west from ~700 mm near Villa Mercedes, to ~370 mm at Chepes and to ~91 mm in San Juan (Compagnucci et al., 2002). A striking characteristic is the seasonal precipitation distribution, with over 70% of precipitation occurring in

austral spring and summer months of October through March (Fig. 3) associated with the southward expansion of the South American Convergence Zone (e.g. Barros and Silvestri, 2002). Mean maximum summer temperatures during this rainy season can often exceed 35 °C, enhancing evaporative losses.

The source of this precipitation and warmth is cyclonic activity spawned from the back circulation of the subtropical South Atlantic anticyclone (Compagnucci et al., 2002) and the low level meridional Chaco Jet which brings warm and moist air derived from tropical jungles and humid lowlands of Bolivia and Brazil southward along the eastern margin of the Andes (Wang and Paegle, 1996; Saulo et al., 2000). The subtropical Andes Mountains with a mean peak elevation of 4000 m are an effective barrier for import of moisture from the Pacific Ocean. A critical synoptic scale element for the import of moisture to central-west Argentina is the pressure gradient between a thermal-orographic but dynamic northwesterly low, located east of the Andes and the subtropical South Atlantic Anticyclone. This pressure gradient increases during the austral summer resulting in northeasterly flow and the net import of moisture from Atlantic Ocean and Bolivian sources. In winter, with less surface heating and northward displacement of westerlies, the import of moisture significantly declines (Compagnucci et al., 2002).

3. Geomorphic, stratigraphic and sedimentologic field approaches

The extent of dune fields, dune types and relation to other geomorphic features was assessed for San Luis, Médanos Negros and Médanos Grandes through detailed examination of a variety of remotely sensed images. Principally two Landsat ETM+images (one acquired on 18 November 2002 and other one, S-19-30_2000, obtained from https://zulu.ssc.nasa.gov/mrsid/) were used to decipher large-scale features and map laterally boundaries of dune fields. Selected aerial photography (scales 1:40,000 to 1:75,000) was also obtained for each dune field and was pivotal for assessing dune type. In turn, extensive field assessment mapped smaller scale geomorphic features.

The movement of eolian sand and the development of dune forms are principally controlled by the strength of winds and the availability and supply of eolian sand for transport (Kocurek and Lancaster, 1999). Wind is not a limiting factor with threshold wind speeds (>5 m/s) for sand movement attained seasonally (Figs. 4C, 7C and 10C). All three dune fields studied in western Argentina

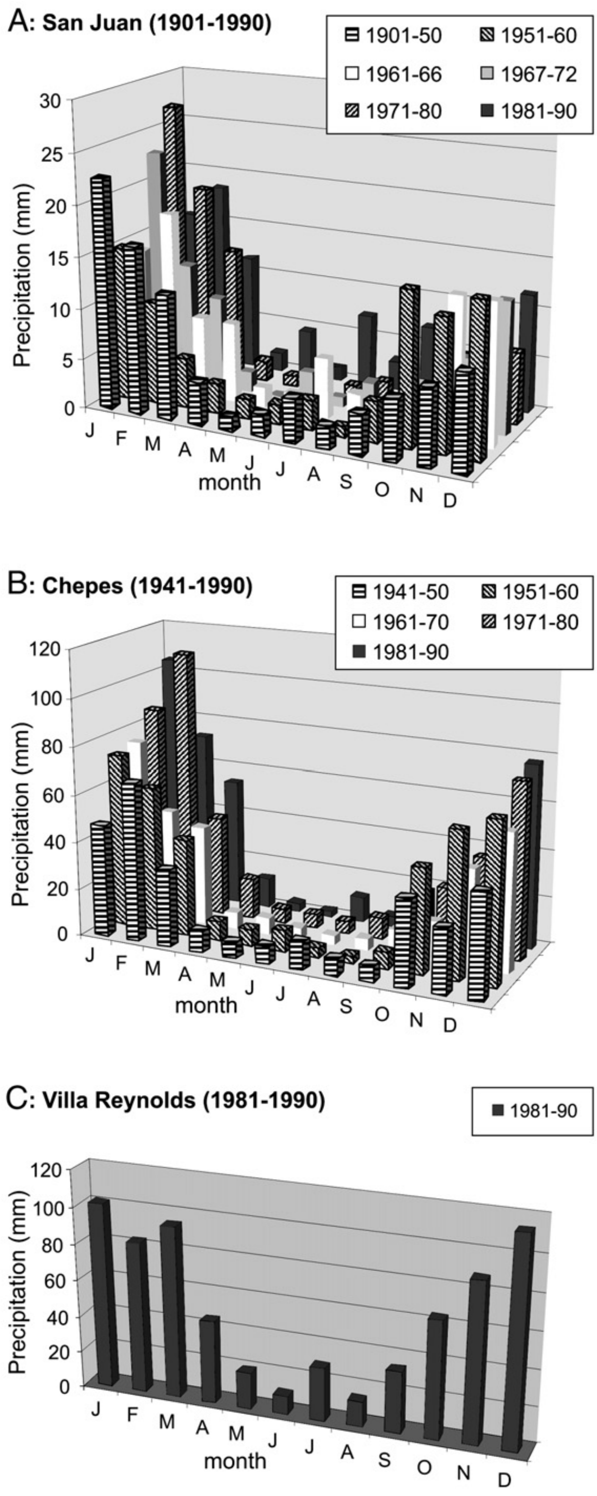

Fig. 3. Seasonal precipitation (mm) variability for weather stations near studied dune fields: (A) Médanos Grandes (San Juan INTA: 31° 37'S, 68° 32'W, 1901–1966/1971–1980; and San Juan Aero: 31° 34'S, 68°25'W, 1967–1990), (B) Médanos Negros (Chepes: 31° 20'S, 66° 35'W, 1941–1990) and (C) San Luis (Villa Mercedes/Reynold: 33° 26'S, 65° 12'W, 1981–1990). Data were from Servicio Meteorológico Nacional, Buenos Aries, Argentina.

are well vegetated and prior activity principally reflects the reduction of vegetation, and thus we suspect these ergs are predominately availability controlled landforms. However, Médanos Grandes, the driest of the dune fields, is eroded and surrounded by large braided fluvial channels and may reflect variability in fluvial sediment supply.

This research focused on deciphering the most recent evidence for eolian activity in western Argentina, which is variably exposed in natural and human-made exposures usually <2 m deep. We recognize that any one stratigraphic locality contains a conservative record of eolian depositional events. Thus, there is the need to examine multiple sections in each dune field, which collectively may reflect the complex history of dune reactivation/formation. In turn, at many localities 10s to 100s of meters of section are laterally exposed allowing us to evaluate the continuity of stratigraphic units. In this study we examine at least two stratigraphic sections in each dune field and because of the limited record assessed to date the resultant environmental assessment is far from complete.

Sections were studied with attention to sedimentologic and pedogenic details. The attitudes of beds were recorded to assess paleowind directions. These measurements are most meaningful where bed dips are >10°. In turn, bed thickness, grading or couplets and granulometry changes were recorded. Attention was carefully focused on bedding planes and unit contacts to assess if there were hiatuses in deposition, indicated by localized mixing (bioturbation). Detailed sedimentologic study of the eolian sediments addresses if eolian deposition is characterized by numerous incremental events or rapid delivery of eolian sand by a few events. Cover sands may be associated with partial reactivation of some dunes and formation of blowout dunes. Larger scale dune reactivation or formation are identified by >4 m accumulation of eolian sand, high to moderate angled (15–30°) cross-stratification, with numerous reactivation surfaces and with little bioturbation reflecting primary dune migration.

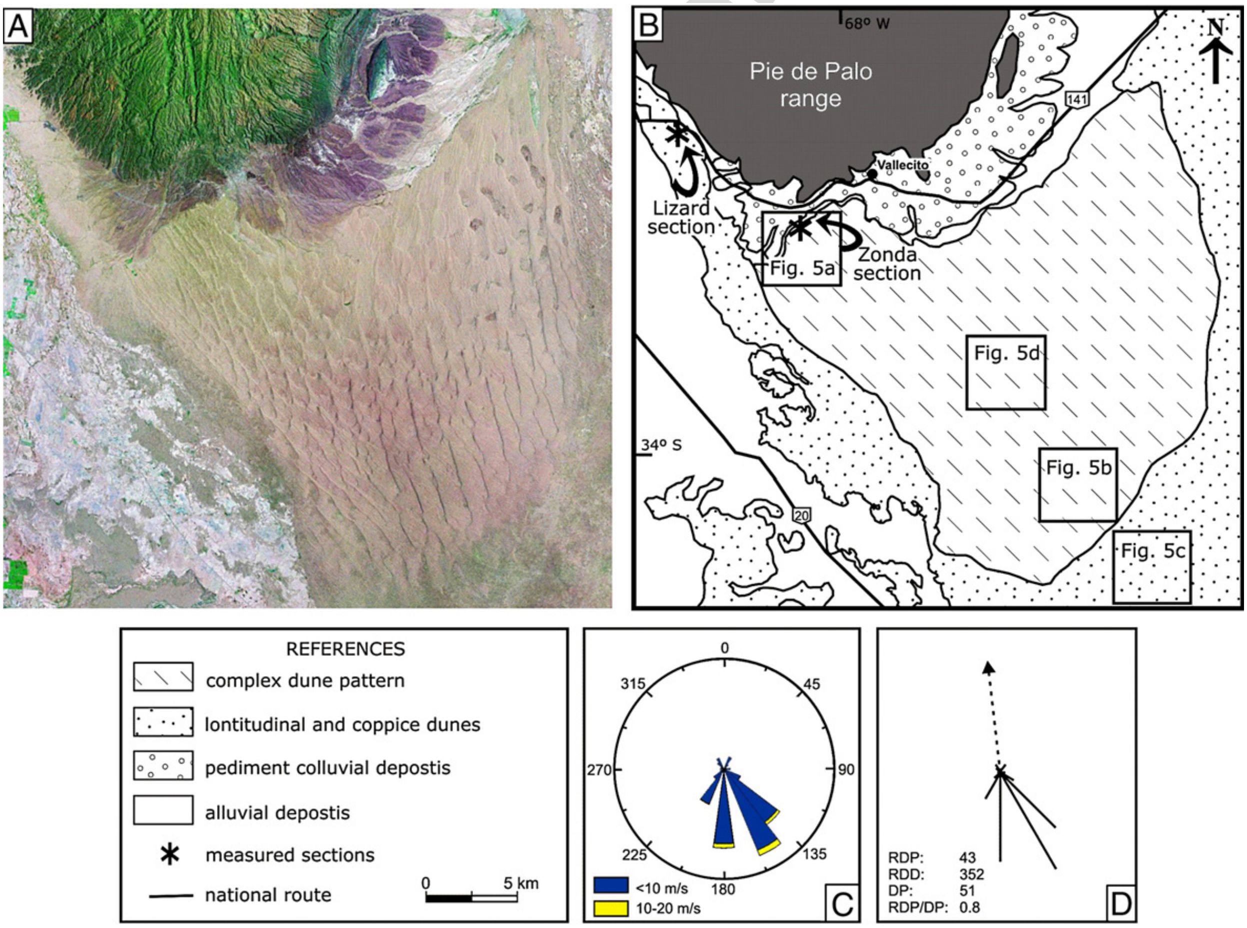

Fig. 4. (A) Enlargement of Landsat ETM+image (bands 7, 4 and 2 of image acquired on 18 November, 2002) and (B) surficial geologic map of Médanos Grandes dune field (San Juan Province, Argentina), (C) wind rose for nearby (~50 km NW) San Juan for January 1, 1995, to December 31, 2004, based on hourly measurements, (D) sand drift potential from vectorial analysis from (C) following Fryberger (1979, p. 147). RDP=resultant drift potential, RDD=resultant drift direction and DP=drift potential.

The recognition and lateral tracing of paleosols is pivotal because this stratigraphic marker reflects landscape stability, associated with relatively moist climate (e.g. Forman et al., 2001). We used standard soil stratigraphic and geomorphic approaches as outlined by Birkeland (1999). Sections were carefully studied to assess lateral variations in soil development to gain insight on how pedogenesis varies across slopes. Eolian stratigraphic units representing discrete depositional events were defined by bounding soils and sedimentologic characteristics. A clear synergy is that OSL dating of eolian sand subjacent and overlying a paleosol provides an estimate of duration of pedogenesis and for relative wet conditions between dry periods.

4. Luminescence dating

The eolian stratigraphy was sampled for luminescence dating only after there is a full understanding of sedimentology, extent of soil development and associated lateral changes. We extracted at least three luminescence-dating samples from each eolian stratigraphic unit, scrupulously avoiding horizons of pedogenesis and favoring primary eolian depositional strata. Sampling for OSL dating use light tight 5-cm-diameter and 15-cm-long sections of black ABS pipe, which were hammered into the desired sampling level.

Optically stimulated luminescence geochronology is based on the time-dependent dosimetric properties of silicate minerals, predominately quartz (Aitken, 1998). Single-aliquot regenerative (SAR) (Murray and Wintle, 2000, 2003) and multiple-aliquot regeneration (MAR) (Singhvi et al., 1982; Jain et al., 2003) protocols were used in this study to estimate the equivalent dose of the 150- to 250-μm quartz fractions from dune sands (Table 1). Eolian sands from western Argentina are often mineralogically immature, consisting of well-sorted medium to fine sand, with median grain sizes ranging from 100 to 250 μm, composed of mafic rock fragments, quartz and other mixed lithologies. The quartz fraction was isolated by density separations using the heavy liquid Na–polytungstate, and a 40-min immersion in HF was applied to etch the outer 10+ μm of grains, which are affected by alpha radiation (Mejdahl and Christiansen, 1994). The purity of the quartz separate was evaluated by petrographic inspection and point counting of a representative aliquot. Samples that showed >1% of non-quartz minerals were retreated with HF and checked petrographically. Duplicate or triplicate reaction with HF was often needed to obtain a pure quartz separate. The purity of quartz separates for selected samples was tested by exposing small aliquots to infrared excitation (880 nm), which preferentially excites feldspar minerals. Samples under infrared excitation showed weak emissions at or near background levels (<300 counts), indicating a spectrally pure quartz extract.

An Automated Risø TL/OSL-DA-15 system (Bøtter-Jensen et al., 2000) was used for SAR and MAR analyses. Blue light excitation (470±20 nm) was from an array of 30 light-emitting diodes that delivers ~15 mW/cm^2 to the sample position at 90% power. A Thorn EMI 9235 QA photomultiplier tube coupled with three 3-mm-thick Hoya U-340 detection filters, transmitting between 290 and 370 nm, measured photon emissions. Laboratory irradiations used a calibrated ^{90}Sr/^{90}Y beta source coupled with the Risø reader. All SAR emissions were integrated over the first 0.8 s of stimulation out of 500 s of measurement, with background based on emissions for the last 90- to 100-s interval.

Before the application of SAR protocols a series of experiments evaluated the effect of preheating at 180°, 200°, 220° and 240 °C on the regenerative signal (Murray and Wintle, 2000). These experiments show that preheat temperatures of 200 °C yielded the highest and consistent equivalent doses, and so aliquots were preheated at this temperature for 10 s for the SAR protocols. Tests for dose recovery were also performed and for samples the last dose coincides well with the initial dose (at one sigma errors).

Multiple-aliquot regenerative ages (Singhvi et al., 1982) were determined on selective samples using the component-specific dose normalization (Table 1), similar to Jain et al. (2003). Laboratory solar resetting of natural luminescence was by an 8-h exposure to 275 w GE Mercury Vapor Sunlamp, which is effective in evicting electrons from photosensitive traps (Richardson, 1994). A normalization dose (~82 Gy β) was applied to all discs prior to analysis and the ratio of secondary to initial luminescence response was used to derive a correction factor for sensitivity changes. The efficacy of the preheat treatment for the normalization dose was evaluated by comparing curve shape (trap distribution) between the natural and subsequent dose. A similar dose response was indicated by zero or low slope (<0.1) between the luminescence for initial and secondary dose evaluated at 1-s intervals. A preheat of 150 °C for 1 h yielded a luminescence distribution most similar to the natural emissions.

A critical analysis for luminescence dating is the dose rate, which is an estimate of the exposure of the sediment to ionizing radiation during the burial period (Table 1). The U and Th content, assuming secular

Table 1
Optically stimulated luminescence ages for eolian sand depositional events for paleo-dune fields Medanos Grande, Medanos Negros and San Luis, western Argentina

Field number	OSL Lab number	SAR aliquots [a]	SAR D_e (Gy) [a]	MAR D_e (Gy) [b]	U (ppm) [c]	Th (ppm) [c]	K_2O (%) [c]	Cosmic dose rate (mGy/years) [d]	Dose rate (mGy/years)	MAR age (years)	SAR age (years)
Medanos Grande											
MG05-06	UIC1719Bl	27	7.55±0.20		2.3±0.1	7.4±0.1	2.57±0.03	0.12±0.01	3.65±0.16		2070±150
MG05-07	UIC1615Bl	29	2.33±0.09		2.4±0.1	9.1±0.1	2.68±0.03	0.14±0.01	3.91±0.17		600±40
MG05-10	UIC1617Bl	36	1.35±0.12		2.1±0.1	7.3±0.1	2.55±0.03	0.14±0.01	3.39±0.15		400±45
MG05-11	UIC1612Bl	30	1.57±0.13		2.1±0.1	8.0±0.1	2.61±0.03	0.18±0.02	3.71±0.16		410±45
MG05-12	UIC1606Bl	26	13.87±1.19		1.6±0.1	5.8±0.1	2.39±0.02	0.10±0.01	3.21±0.15		4300±500
MG05-15	UIC1716Bl	30	13.11±0.66		1.8±0.1	6.9±0.1	2.37±0.02	0.10±0.01	3.27±0.15		4005±320
MG05-18	UIC1604Bl	28	13.36±0.68		1.6±0.1	5.8±0.1	2.48±0.03	0.12±0.01	3.27±0.15		4090±335
Medanos Negros											
MN05-01	UIC1605Bl	29	1.79±0.08		0.9±0.1	3.7±0.1	1.51±0.02	0.15±0.02	1.98±0.09		900±70
MN05-03	UIC1713Bl	23	0.81±0.11		0.9±0.1	4.2±0.1	1.37±0.01	0.19±0.02	1.93±0.09		400±65
MN05-04	UIC1720Bl	26	4.71±0.34		0.9±0.1	4.4±0.1	1.28±0.02	0.18±0.02	1.90±0.09		2540±240
San Luis											
SL05-19	UIC1608IR			96.86±0.17	2.3±0.1	9.4±0.1	2.74±0.03	0.13±0.01	3.54±0.16	27,330±2080	
SL05-19	UIC1608GR			96.36±3.29	2.3±0.1	9.4±0.1	2.74±0.03	0.13±0.01	3.54±0.16	27,185±2280	
SL05-22	UIC1613GR			90.59±0.19	2.1±0.1	7.9±0.1	2.57±0.03	0.15±0.02	3.67±0.16	24,700±1500	
SL05-23	UIC1610Bl	30	0.26±0.01		2.5±0.1	9.4±0.1	2.88±0.03	0.12±0.01	4.04±0.17		65±5
SL05-25	UIC1616IR			122.97±1.06	2.4±0.1	8.9±0.1	2.79±0.03	0.13±0.01	3.76±0.16	32,700±2150	
SL05-26	UIC1607Bl	28		91.19±3.87	2.5±0.1	9.0±0.1	2.87±0.03	0.14±0.01	3.88±0.17		23,500±1830
SL05-26	UIC1607IR			97.29±0.09	2.5±0.1	9.0±0.1	2.87±0.03	0.14±0.01	3.88±0.17	25,090±1630	
SL05-26	UIC1607GR			107.23±4.07	2.5±0.1	9.0±0.1	2.87±0.03	0.14±0.01	3.88±0.17	27,650±2085	
SL05-27	UIC1714BL	29	0.35±0.01		2.3±0.1	7.9±0.1	2.66±0.03	0.17±0.02	3.67±0.16		95±10
SL05-28	UIC1611Bl	30	0.26±0.03		2.2±0.1	8.2±0.1	2.78±0.03	0.18±0.02	3.95±0.17		70±10
SL05-29	UIC1715Bl	28	0.33±0.003		2.2±0.1	7.6±0.1	2.70±0.03	0.16±0.02	3.78±0.17		90±10
SL05-31	UIC1609Bl	28	0.060±0.003		2.1±0.1	7.5±0.1	2.60±0.03	0.18±0.02	3.78±0.17		15±2

[a] SAR, single-aliquot regeneration protocols used for equivalent dose (D_e) determination (Murray and Wintle, 2003; Olley et al., 2004), under blue light (Bl) excitation (470±20 nm).
[b] MAR, multiple-aliquot regeneration procedures used equivalent dose (D_e) determination (Jain et al., 2003): IR = infrared excitation (880±80 nm), GR = green light excitation (514±20 nm).
[c] U, Th and K_2O content determined by ICP-MS by Activation Laboratory Inc. Ontario, Canada.
[d] From Prescott and Hutton (1994).

equilibrium in the decay series and ^{40}K, are determined by inductively coupled plasma-mass spectrometry (ICP-MS) analyzed by Activation Laboratory LTD, Ontario, Canada. The beta and gamma dose was adjusted according to grain diameter to compensate for mass attenuation (Fain et al., 1999). A small cosmic ray component between 0.19 and 0.13 ± 0.01 mGy/years, depending on depth of sediment, was included in the estimated dose rate (Prescott and Hutton, 1994).

In this study both MAR and SAR dating protocols are used and are complimentary geochronologic approaches. The SAR method is preferentially used on eolian sands <10,000 years old because of its proven sensitivity for dating recent (100 to 1000 years old) eolian sand (e.g. Goble et al., 2004; Forman et al., 2005, 2006). The MAR method yields a non-saturated response for older sediments and is preferentially used for eolian sand associated with the LGM. Both analytical approaches were used on one representative sample (UIC1607), yielded ages that overlap at one sigma and thus are statistically similar (Table 1). All optical ages are in years prior to AD 2000.

5. The Médanos Grandes Dune Field

The Médanos Grandes Dune Field is one of the largest and tallest intermountain eolian systems in Argentina (Tripaldi, 2002b), located 30 km southeast of San Juan (Fig. 2). This erg covers an area of 732 km^2 bounded by the Pie de Palo Range to the north, a 3,100-m tall massif composed of Precambrian–Early Paleozoic rocks and is truncated or partially buried by colluvial and fluvial

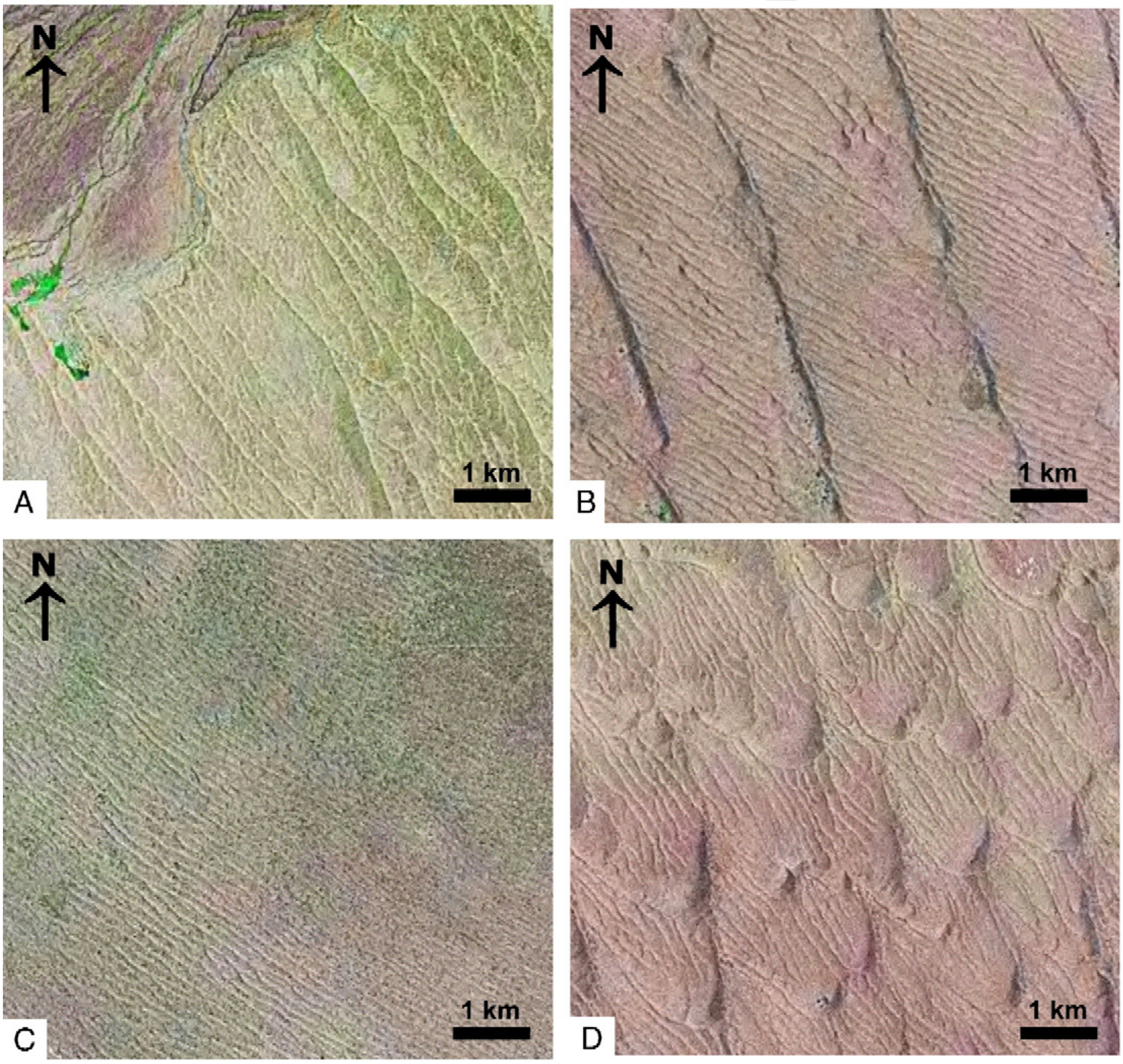

Fig. 5. Eolian landforms recognized in Médanos Grandes dune field (A) Large linear or reverse dune with superimposed smaller dune forms, (B) high parallel ridges with superimposed smaller dunes forming a complex dune-field pattern, (C) linear dunes, (D) large blowout dunes (see Fig. 4 for location).

deposits along other margins (Fig. 4B). This is the driest of the three studied dune fields with a mean annual precipitation of 91 mm/years and >80% of the precipitation occurring between October and March (1901–1990, Fig. 3A). Austral summer temperatures can often exceed 40 °C (Servicio Meteorológico Nacional, 1958a,b, 1969, 1975, 1986, 1994). Wind data collected hourly west of the dune field in San Juan from January 1, 1995, to December 31, 2004, show a strong south to southwesterly component (Fig. 4C). The resultant drift potential (RDP), a measure of the net winds capable of moving sand, is due north at 352° (Fig. 4D) (Fryberger, 1979, pp. 147–152). The vegetation cover is dispersed and dominated by shrubs and short grasses with scatter trees, which hinder the wind transport of sand.

There are a variety of dune forms of various scales in the Médanos Grandes dune field (Fig. 5). The largest landform of presumably eolian origin are up to 50-m high parallel ridges, spaced between 0.25 and >1.5 km and exceeding 5 km in length (Fig. 5a). Some of the large ridges appear to be linear or reverse dunes, especially in the northwestern area where these landforms show a preferred orientation of NNW to SSE (Figs. 4A and 5A), consistent with the wind data (Fig. 4C). However, the ridges in the northern area are clearly asymmetric (transverse dunes) with steeper sides facing NNE. Whereas in the southern region the steep face is exposed to SSW, indicating opposing wind directions (Fig. 5B). Smaller, linear dunes and orientated NW to SE are superimposed on these ridges (Fig. 5a and b). This complex assemblage of superimposed dune forms at a variety scales may indicate multiple episodes of eolian deposition /reactivation (Lancaster, 1999; Kocurek and Ewing, 2005).

The complex dune forms of Médanos Grandes dune field are surrounded by a lower relief, rolling surface formed mainly by linear dunes, orientated from N–S to NW–SW, coherent with the wind data (Figs. 4A and 5C). This surface has been subsequently reworked by coppice dunes (Fig. 4). Large blowout dunes also occur in the central area of Médanos Grandes paleo-dune field (Fig. 4). These dunes are up to 1000 m of diameter and up to 50 m deep, with asymmetric hollows indicating paleowinds from the southeast, consistent with 352° RDP (Fig. 5D).

5.1. Stratigraphic sections and chronologic control at Médanos Grandes paleo-dune field

5.1.1. The Lizard Section (31° 41.957′ S; 68° 09.76′ W)

The Lizard Section (Fig. 6) is on the western margin of dune field that reflects regional eolian inputs and clastic sediments from alluvial fans sourced from the adjacent Pie de Palo Range. The basal unit (L1) in this section is a well exposed, poorly sorted deposit of rounded to subrounded pebbles, cobbles and boulders within a coarse sand matrix. This gravel is traceable for 100 m around the quarry, at least 12 m thick and exhibits large-scale, meters-thick, horizontal-to-sub-horizontal stratification. This large-scale unit is predominately composed of dark grey schist, higher grade metamorphic lithologies and noticeable quartz cobbles reflecting a provenance from alluvial fans sourced in the nearby Pie de Palo Range. Overlying unit L1 is a medium-to-coarse moderately well-sorted dark yellowish-brown (10YR4/3.5) sand with scattered 2- to 3-cm-diameter pebbles that increase in concentration in the basal 5–10 cm. This much finer unit (L2) compared to unit L1 reflects distal alluvial fan deposition.

Units L3 to L6 primarily reflect eolian depositional processes. The lowest unit (L3) exhibits evidence for some colluvial contributions, whereas unit L6 is wholly of eolian in origin. Unit L3 is a massive, fine to very fine, brown (10YR5/2.5) sand with common dispersed coarse sand and granules. Disseminated $CaCO_3$ is common in the upper 30 cm of unit L3, where very fine sand lenses predominate. Conformably overlying unit L3 is a complex sedimentary unit (L4) with yellowish-brown (10YR5/4), very fine sand and brown (10YR5/3) silty very fine sand mm-to-cm horizontally laminated interbeds. Silt beds exhibit disruptions from root traces and diffusive lower boundaries associated with pedogenesis and burrowing, particularly in the upper 10 cm. Unit L5 is a yellowish-brown (10YR5/4) massive very well sorted fine sand, approximately 0.5 m thick and unconformably truncates subjacent unit L4. The youngest sediment identified and expressed at the surface as linear dunes is unit L6, which is a very well sorted yellowish-brown (10YR5/4) fine-to-medium sand. Unit L6 exhibits distinctive mm-to-cm scale laminations, including horizontal and high and low angle crossbeds. OSL ages (Table 1) for quartz extracts from units L3, L4, L5 and L6 indicate the respective depositional age of 2070±150 (UIC1719Bl), 600±40 (UIC1615Bl), 400±45 (UIC1617Bl) and 410±45 years (UIC1612Bl).

5.1.2. The Zonda Section (31° 46.207′ S; 68° 02.304′ W)

The Zonda Section is a massive 20-m high vertical section cut into eolian sand by a meander bend of one of the ephemeral rivers that flows into the dune field from the adjacent Pie de Palo Range, with significant reworking and deposition of a cliff-edge dune (Fig. 6). The basal 12 m of this section exposes a linear dune that is expressed at the

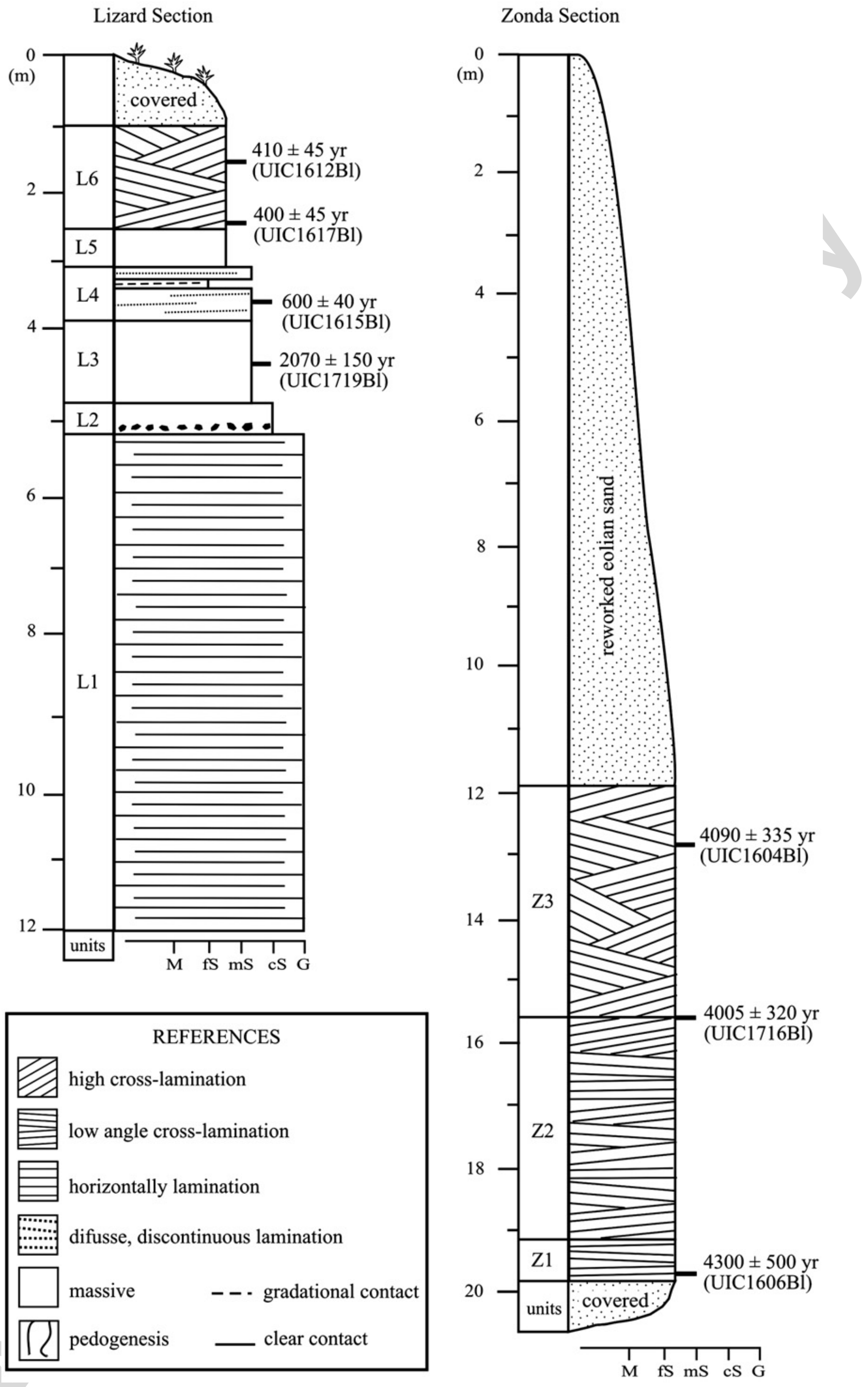

Fig. 6. The Zonda and Lizard stratigraphic sections in Médanos Grandes dune field (see Fig. 4 for location).

surface. Stratigraphic units (Z1, Z2 and Z3) are principally designated by distinct bedding characteristics. The lowest unit (Z1) is a very well sorted, dark yellowish-brown (10YR 4.5/5) medium-to-fine sand, with mm-to-cm horizontal to subhorizontal scale bedding. Beds have been variably disrupted by burrowing. The top contact of unit Z1 is unconformable with a clear 20- to 30-cm-deep scourer surface eroded into the subjacent sand. Unit Z2 is a dark yellowish-brown, very well sorted, medium-to-fine sand, dominated by low-angle bedding. Massive and high-

angle beds also occur in this unit; the latter infills the scoured surface at the basal contact. The uppermost unit (Z3) is a very well sorted, dark yellowish-brown, medium-to-fine sand with distinctive high-angle crossbeds. These crossbeds are thicker (1–1.5 m) in the basal 1 to 2 m with inferred paleowind directions from the N–NE and S–SW. Quartz grains from the basal 0.5 of unit Z1 and the upper 1 m of unit Z3 yielded the corresponding luminescence ages of 4300±500 (UIC1606Bl), 4005±320 years (UIC1716Bl) and 4090±335 years (UIC1604Bl) (Table 1).

6. The Médanos Negros paleo-dune field

Médanos Negros paleo-dune field (Fig. 2) covers an area of 1000 km^2 and is bounded by alluvial deposits to the north and east and by the saline Mascasín Lake (Salinas de Mascasín) (Fig. 7A and B). Dune forms have encroached on to the dried lake basin. The western margin of the erg are the Valle Fértil and de Guayaguas Ranges, containing Precambrian–Early Paleozoic plutonic and metamorphic rocks capped by Triassic–Cretaceous sedimentites (Fig. 7).

Médanos Negros dune field receives about four time the precipitation (~370 mm) of Médanos Grandes, with >85% occurring from October to March (Fig. 3B) coincident with maximum temperature of 31.7 °C. This mesic climate results in a dense vegetation cover of shrubs and trees casting abundant shadows and giving a dark appearance (thus, the name 'Negros'). Wind data collected three times daily (9 am, 3 pm, 9 pm) from Chepes, northeast of the dune field, from January 1, 1995, to December 31, 2004, show a strong northeasterly component (Fig. 7C). The resultant drift potential (RDP) is almost due south at 180° (Fig. 7D) (Fryberger, 1979, pp. 147–152).

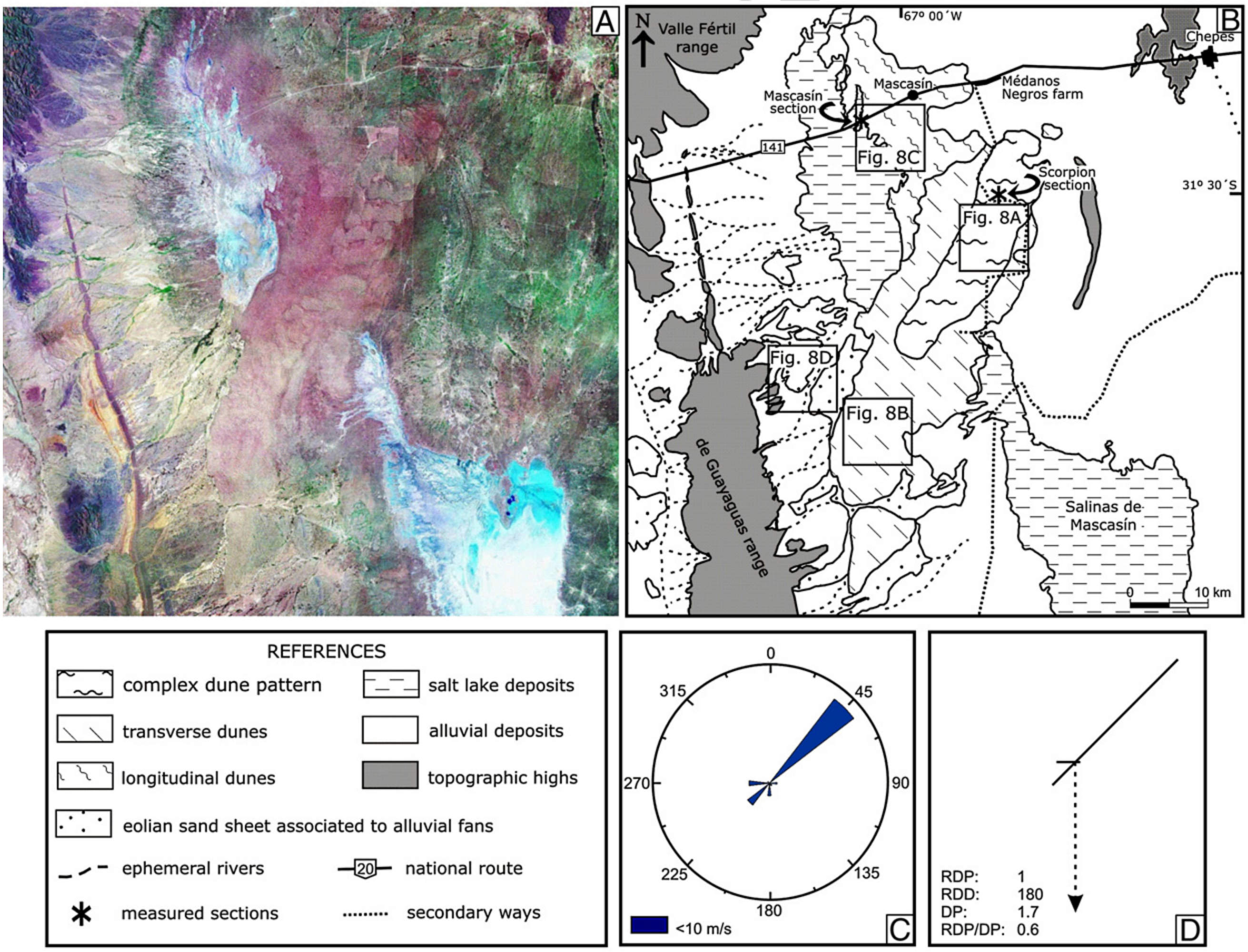

Fig. 7. (A) Enlargement of Landsat ETM+image (bands 7, 4 and 2 of image acquired on 18 November, 2002) and (B) surficial geologic map of Médanos Negros dune field (La Rioja Province, Argentina), (C) wind rose for nearby (~30 km E) Chepes for January 1, 1995, to December 31, 2004, based on three times daily measurements, (D) sand drift potential from vectorial analysis from (C) following Fryberger (1979, p. 147). See Fig. 4D for explanation of abbreviations.

Médanos Negros paleo-erg shows a complex suite of dune-like landforms of various scales, suggesting a compound history of eolian construction/reactivation (Lancaster, 1999; Kocurek and Ewing, 2005). The largest landform is a regular pattern of west-to-east oriented ridges and troughs spaced ~2–4 km apart (Figs. 7 and 8A). This rolling landscape has about 50 m of relief with asymmetric ridges showing steeper sides facing south, similar to large transverse dunes (draa forms of Havholm and Kocurek, 1988). These larger landforms are variably preserved, incised by drainages and covered in places by coarse colluvium. Superimposed on this undulating topography are 5–10 m high, transverse dunes facing SSW to SW (Fig. 8A). Transverse dunes extend beyond the host landforms, to the west and the south in the dune field, trending NW to SE with sinuous crests and often highly modified by coppice dunes (Fig 8B). Linear dunes that are 3–5 m high, 20–30 m wide and 100 m long commonly occur in the northeast and are deposited on and presumably sourced from subjacent salt-rich lake deposits (Fig. 8C). A sand sheet deposit occurs farther to the southwest, associated with alluvial fans emanating from the de Guayaguas Range (Fig. 8D).

6.1. Stratigraphic sections and chronologic control at Médanos Negros paleo-dune field

Stratigraphic sections in Médanos Negros were somewhat difficult to locate on this well vegetated

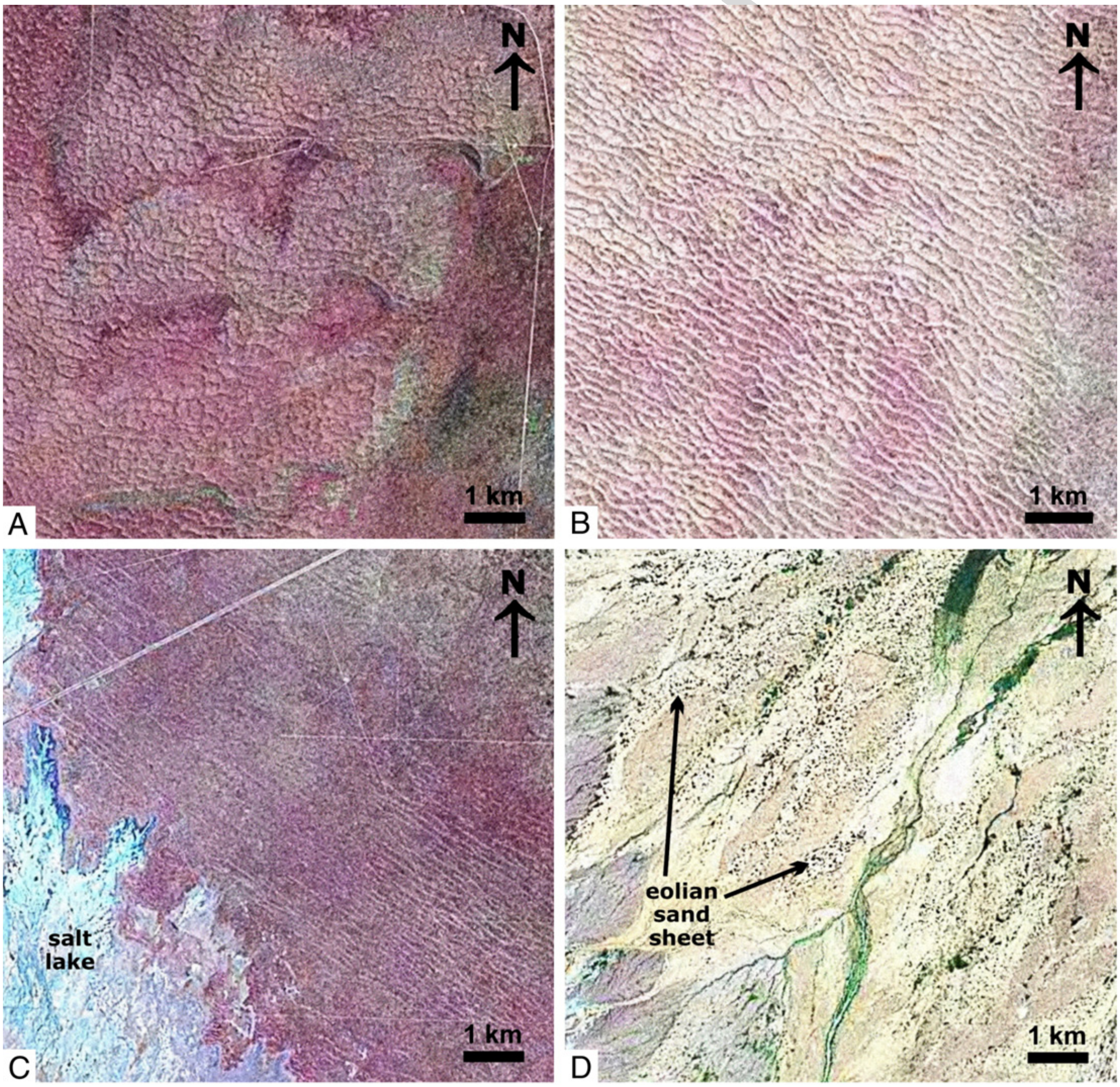

Fig. 8. Eolian landforms recognized in Médanos Negros dune field: (A) high parallel ridges with superimposed smaller dunes forming a complex dune-field pattern, (B) transverse dunes, (C) linear dunes and salt-rich lake deposits, (D) sand sheet forms associated with alluvial fans (see Fig. 7 for location).

landscape. Two sections were studied. The first section (Mascasín) is a barrow pit into linear dunes that formed on salt-rich lake deposits (Figs. 7B and 9). The second, the Scorpion Site, is an excavation into transverse dunes in the dune mass (Figs. 7B and 9). These transverse dunes show 6 to 8 m relief and are noticeably asymmetric, with many steep sides facing southwest.

6.1.1. The Mascasín Section (31° 25.414′ S; 67° 02.867′ W)

Three meters of eolian sand is exposed at this locality, reflecting the last period(s) of linear dune migration (Fig. 9). Two distinct sedimentary units are recognized. The basal unit (M2) is a very well sorted brown (10YR 4.5/3) fine sand, mostly massive with abundant medium-to-coarse sand sized intraclasts of salt-rich (NaCl and $CaSO_4$) sediment. The upper unit (M1) is a very well sorted fine-to-medium sand, with low angle and mm-scale bed remnants, disrupted by bioturbation (unit M1A). The upper 1 m, unit M1B, shows clearer bedding in places with mm-to-cm scale low angle crossbedding and distinct redder colors (7.5YR5.5/4). Bed remnants have an apparent sense in the north to south plane. The lower part of unit M2 yielded the luminescence age of 900±70 years (UIC1605Bl), whereas eolian sand from 1 m depth (unit M1B) gave the age of 400±65 years (UIC1713Bl).

6.1.2. The Scorpion Site (31° 30.204′ S; 66° 51.915′ W)

This site is a shallow excavation (~2 m) into a well stabilized and heavily vegetated transverse dune crest. One stratigraphic unit is recognized, which is a yellowish-brown (10YR4.5/4) very well-sorted fine sand (Fig. 9). This sand is mostly massive in the upper 1 m reflecting pedogenic mixing. However, in the lower 30 to 40 cm this unit shows distinct 10- to 30-cm-long mm-scale bed remnants with redder colors (7.5YR5/4). The surface soil shows particularly weak development with just the presence of 5-cm-thick A horizon. Luminescence dating of quartz grains from bed remnants at 1.7 m yielded the age of 2540±240 years (UIC1720Bl).

7. The San Luis paleo-dune field

Most of the southern half of San Luis Province is mantled by well vegetated and stabilized dunes and eolian sands (Fig. 10A and B), here named the San Luis paleo-dune field (Fig. 2). These eolian deposits are part

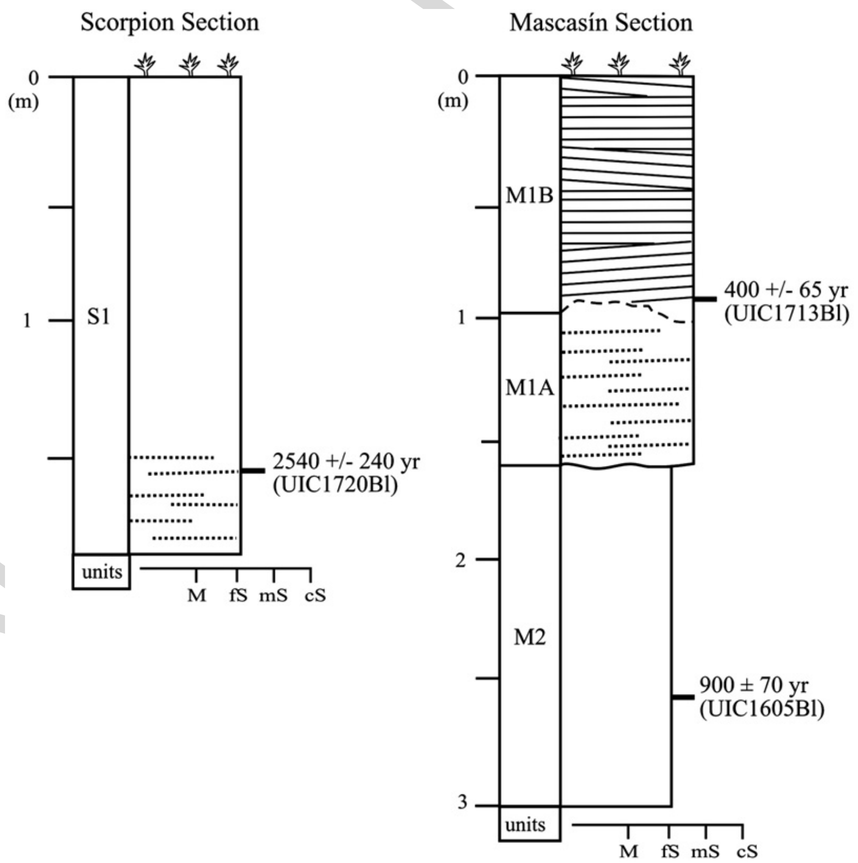

Fig. 9. Scorpion and Mascasín stratigraphic sections in Médanos Negros dune field (see Fig. 7 for location and Fig. 6 for references).

of an inferred larger Late Quaternary eolian system, the "Pampean Sand Sea" (e.g. Iriondo and Kröhling, 1996; Iriondo, 1999) that cover most of central Argentina (Fig. 1). The San Luis paleo-dune field is the wettest of the three dune fields studied with ∼700 mm precipitation during the rainy season (November–March) (Fig. 3C) and a mean temperature of 17 °C (National Weather Service, 1986). This mesic environment supports Savannah-type vegetation with surface soils with well developed and organic rich A horizons. Wind data collected hourly from 6 am to 9 pm from Villa Reynolds, north of the dune field (Fig. 10C), from January 1, 1995, to December 31, 2004, show dispersed components from the northeast to the southeast (Fig. 10C). The resultant drift potential (RDP) are to the north-northwest at 329° (Fig. 10D) (Fryberger, 1979, pp. 147–152). Our studies focus on the northern area of San Luis dune field, located 15 km to the SW of Villa Mercedes (Fig. 2).

This dune field is characterized by a mantle of eolian sands that show different degrees of deflation and eolian reworking in the form of blowouts and small parabolic dunes. Four distinctive eolian landscapes have been distinguished in this area through analysis of satellite images and aerial photographs and field survey (Fig. 10). This landscape has <4 m of relief from incipient blowouts that erode into the subjacent horizontal laminated, well-sorted sand (medium) sheet (Fig. 11A). The western part of the studied area is characterized by simple, elongate parabolic dunes that average 900 m in length and 250 m in width (length/width ratios >3; Fig. 11B). Dune orientation indicates paleo-winds mostly from the southeast, consistent with wind data (Fig. 10C). Compound and digitate parabolic dunes are common throughout the dune field (Fig. 11C). These dunes average 2000 m in length and 1130 m in width and are also formed by winds mostly from the southeast. Incipient superimposed parabolic dunes occur on dune noses and upper arms. Shallow blowouts, ∼250 m diameter, are also scattered among the parabolic dunes. An eolian landscape principally composed of active,

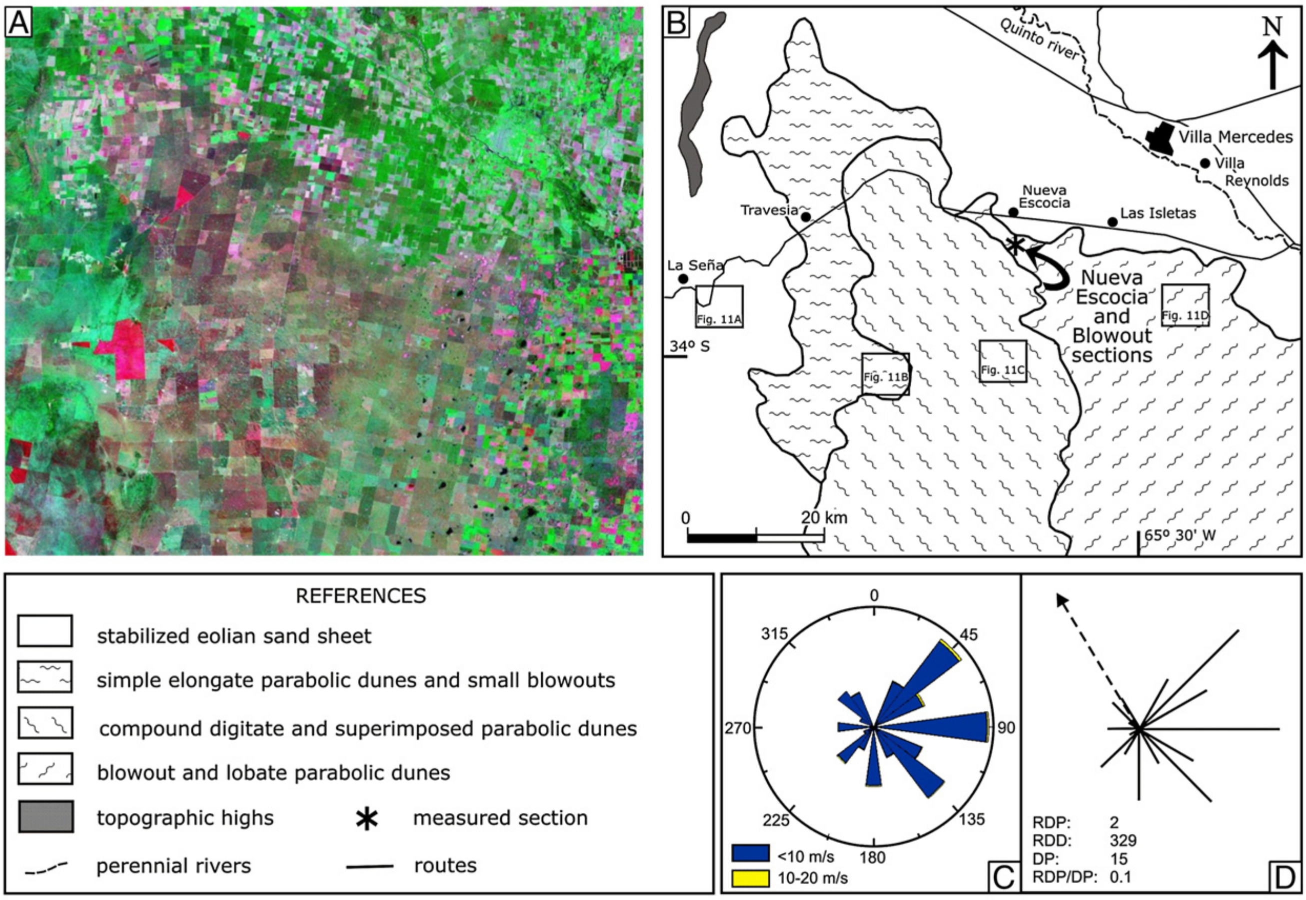

Fig. 10. (A) Enlargement of Landsat ETM+image (bands 7, 4 and 2 of image S-19-30_2000) and (B) surficial geologic map of San Luis dune field (San Luis Province, Argentina), (C) wind rose for nearby (∼30 km E) Villa Reynolds for January 1, 1995, to December 31, 2004, based on hourly, from 6 am to 9 pm, daily measurements, (D) sand drift potential from vectorial analysis from (C) following Fryberger (1979, p. 147). See Fig. 4D for explanation of abbreviations.

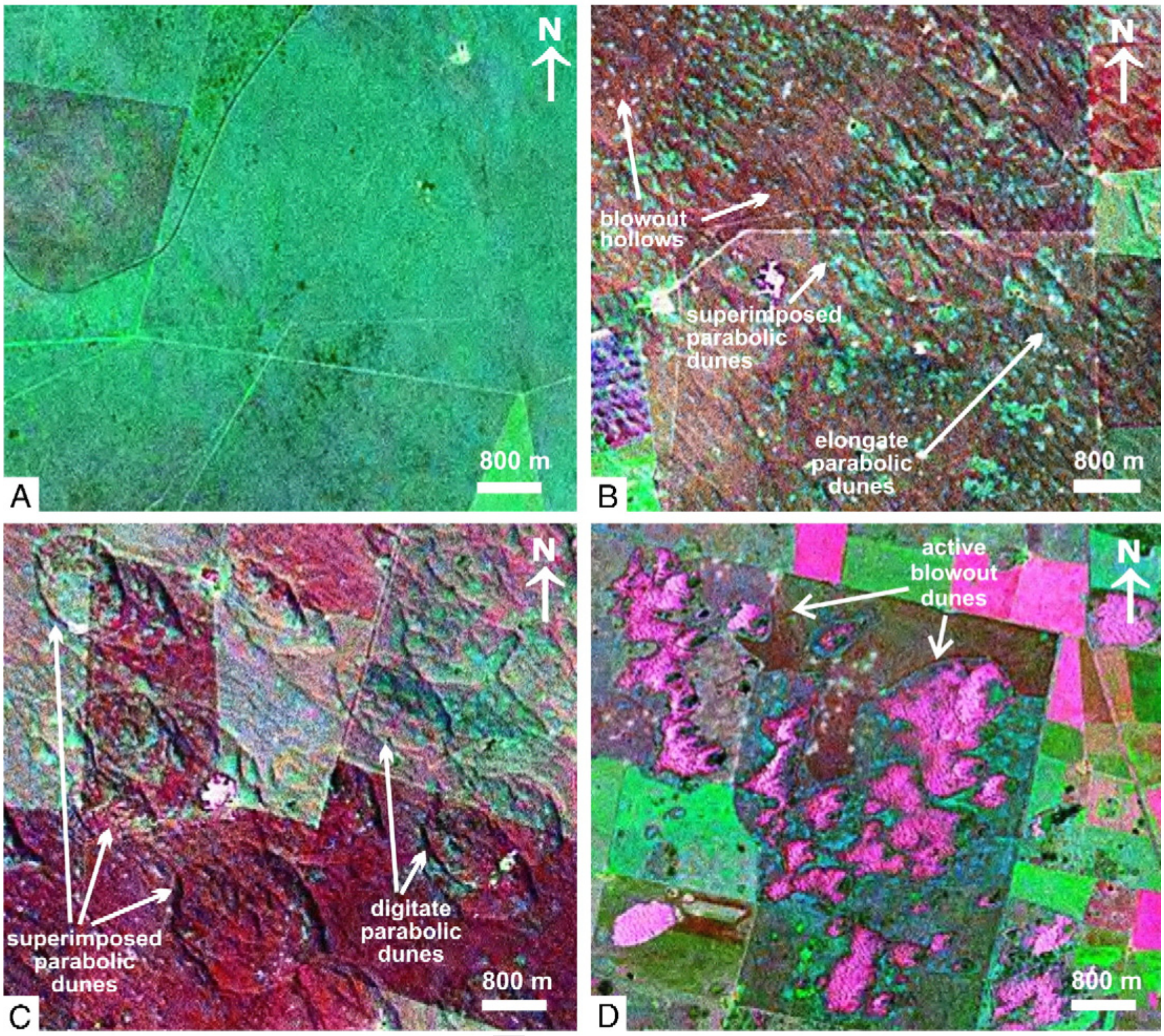

Fig. 11. Eolian landforms recognized in San Luis dune field: (A) stabilized eolian sand sheet, (B) simple elongate parabolic dunes and small blowouts, (C) compound digitate and superimposed parabolic dunes, (D) blowout and lobate parabolic dunes (see Fig. 10 for location).

irregular blowouts with some parabolic dunes characterize the eastern margin of the paleo-dune field (Fig. 11D). These landforms are readily distinguishable by the presence of large and irregular surfaces of loose sands associated with eolian bedforms. Blowouts vary from nearly circular to irregular hollows, from tens of meters to up to 1.5 km long, surrounded by depositional lobes. Blowout depressions, including

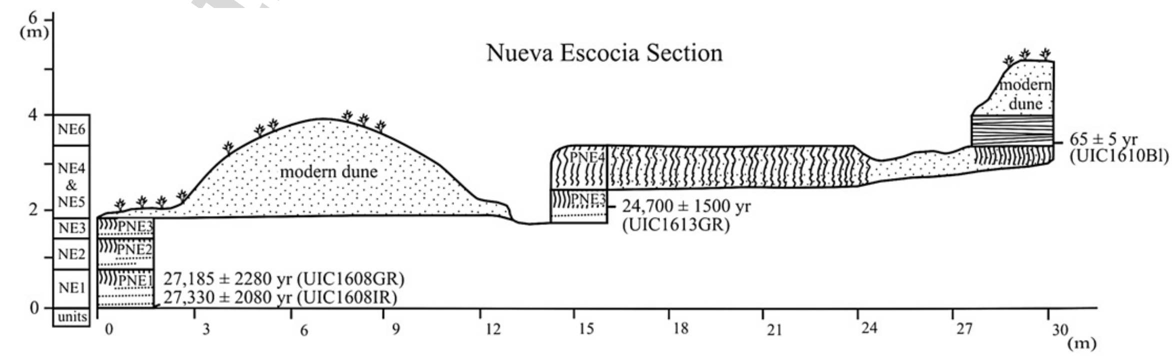

Fig. 12. Nueva Escocia stratigraphic section in San Luis dune field (see Fig. 10 for location and Fig. 6 for references).

many that are compound, are often infilled with water forming perennial lakes. Some lobate parabolic dunes also appear in this area, showing perennial lakes in their deflation troughs. Superimposed on these lobate parabolic dunes are smaller blowout dunes, formed by winds from the northeast. The presence of extensive surfaces with actively migration sand, bordering blowout dunes, reflects the youngest eolian processes in the San Luis dune field. This inferred last dune movement is associated with winds mostly from the northeast (Fig. 10C).

7.1. Stratigraphic sections and chronologic control at paleo-San Luis dune field

Sections for the San Luis paleo-dune field are confined to a large compound blowout formed from northeasterly winds (Fig. 10). We studied two sections that expose a complex sequence of eolian sands and paleosols (Figs. 12 and 13).

7.1.1. Nueva Escocia Section (33° 49.197′ S; 65° 43.322′ W)

This section contains four paleosols, with a range of development, separated by eolian sand. The basal 3 eolian units (NE1, NE2 and NE3) are characterized by yellowish-brown (10YR5/4) to brown (7.5YR4/4), very well-sorted medium-to-fine sand, with horizontal to subhorizontal mm-to-cm scale bed remnants common. The three intervening paleosols are truncated by the emplacement of the overlying eolian sands and exhibit cambric B horizons. The lowest paleosol (PNE 1) shows the most extensive pedogenesis with a 60-cm-thick dark brown (10YR 4/3) cambric horizon, well-developed structure (subangular) and abundant rhizoliths. The uppermost soil exhibits the weakest pedogenesis with a juvenile cambric horizon and weak structure. The two uppermost units (NE4 and NE5), mostly dominated by pedogenesis, are 11 m disjunct from the lower three units (Fig. 11), but remnants of paleosol PNE 3 are identified and serve to correlate subsections. Paleosol PNE 4 exhibits well-developed, cumulic, cambric horizons and is welded with subjacent paleosol 3 such that relatively unaltered, very well sorted medium sand only occurs below paleosol 3. The top of paleosol PNE 4 has been truncated and a variety of subfossils have been concentrated, including bird bones, rodent teeth, jaws and bones. Unconformably overlying paleosol PNE 4 are loose stratified sand, forming the surface slope at 20–25°. Quartz grains from pedogenically unaltered eolian sand from unit NE1 yielded luminescence ages (Table 1) of 27,330±2080 years (UIC1608IR) and 27,185±2280 years (UIC1608GR) while those from sand from unit NE3 gave an age of 24,700±1,500 years (UIC1613GR). Finally, unit NE6, the surface sand, yielded the luminescence age of 65±5 years (UIC1610Bl).

7.1.2. Blowout Section (33° 49.178 S, 65° 43.343′ W)

The Blowout Section is 20 m north of Nueva Escocia Section, which exposes over 10 m of eolian sand in two disjunct but readily correlated sections (Fig. 13). The lowermost unit (B1) is mostly pedogenically altered hosting a well-developed 70-cm-thick buried, strong brown (7.5YR4.5/6) cambric horizon and abundant rhizoliths. Below this paleosol within the basal 20 cm of

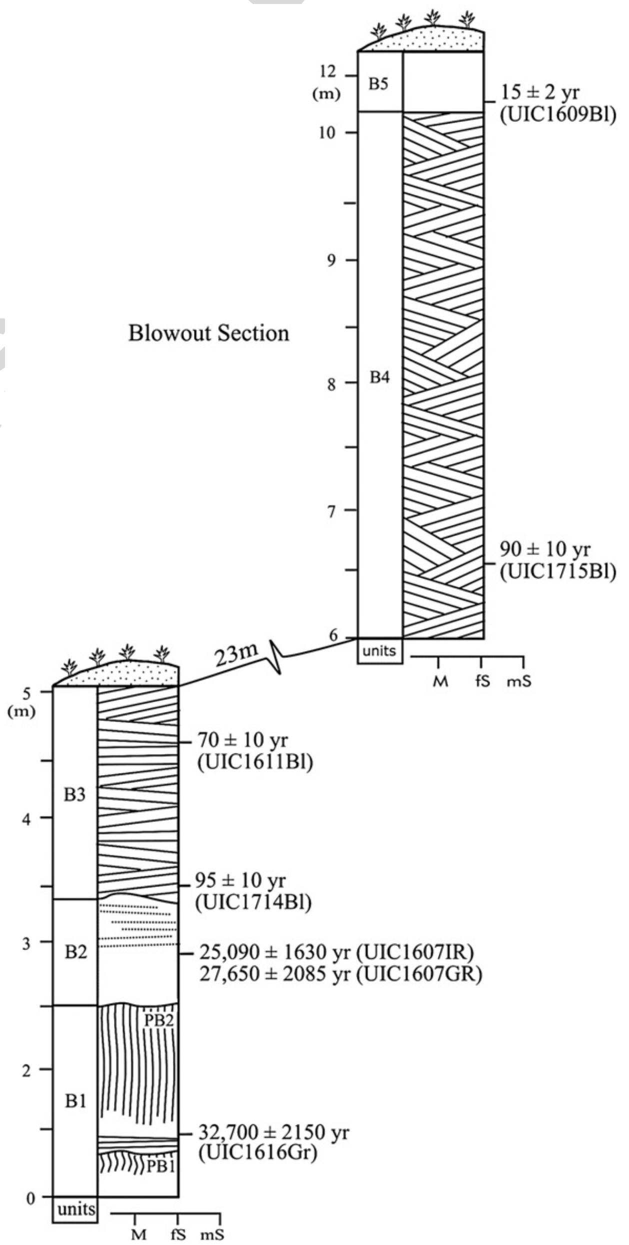

Fig. 13. Blowout stratigraphic section in San Luis dune field (see Fig. 10 for location and Fig. 6 for references).

unit B1 is an unweathered dark yellowish-brown (10YR4.5/6), very well sorted fine sand. This paleosol has been truncated by the deposition of the overlying unit (B2), which is a very well sorted fine sand, with faint horizontal laminations, disrupted by burrowing. The overlying B3 unit is dark yellowish-brown (10YR4/5) well sorted medium sand, with abundant cm-scale coarse sand lenses, and shows a variety of eolian sedimentary structures. The lower 40 cm exhibits horizontal to low-angle (~5°) coarse and medium sand beds, many inversely graded, indicating ripple bed migration. Coarse sand lens predominate and have lower erosional boundaries, with concave or convex forms, consistent with a migrating bedform. Bedding thins to mm-scale at 4 m depth with inversely graded low-angle cross lamination. In the upper 0.5 m of unit B3 bedding further thins and is undulatory, reflecting the presence of vegetation with a migrating sand sheet. The upper part of the Blowout Section is 23 m northwest of the lower section exposed in a higher blowout. At the base of this blowout is a very well sorted fine-to-medium sand (unit B4) with common lenses of medium-to-coarse sand forming high angle crossbeds. Individual beds are mm-to-cm in scale, and many coarse sand beds are asymptotic down the bedding plain, reflecting grain flow. Reactivation surfaces are common and either have concave or convex forms indicating active dune and bedform migration. The upper most unit, capping the section, is a very well sorted fine sand with low angle to horizontal bedding that truncates subjacent high angle beds.

The Blowout Section yielded a wide range of luminescence ages (Table 1; Fig. 13). The basal unit B1 yielded the oldest luminescence age of 32,700±2150 (UIC1616IR), with the overlying unit B2 giving ages of 27,650±2080 years (UIC1607GR) and 25,090±1630 years (UIC1607IR). Units B3 and B4 yielded the surprisingly young ages of 70±10 years (UIC1611Bl), 90±10 years (UIC1715Bl) and 95±10 years (UIC1714Bl) with the uppermost unit B5 dated to 15±2 years (UIC1609Bl).

8. Late Quaternary eolian depositional events in western Argentina

The eolian stratigraphy and associated optical ages for the disjunct San Luis, Médanos Negros and Médanos Grandes dune fields indicate several potential eolian depositional events of unknown magnitude and continuity in western Argentina during the Late Quaternary. Five broad episodes of eolian sand deposition are identified including (1) during the Last Glacial Maximum, (2) ca. 4 ka, (3) ca. 1 ka, (4) 15th to 17th centuries and (5) within the past 100 years (Fig. 14). The eastern-most San Luis dune field contains the sole evidence for eolian deposition during the LGM with cover sands and intercalated paleosols that span ca. 33 to 22 ka. These oldest eolian sands are partially coeval with loess deposition on the Pampas (Zárate, 2003 and references therein; Kemp et al., 2004a,b) and reflect sand sheet deposition, associated with the latest development of the "Pampean Sand Sea" (Iriondo and Kröhling, 1996; Kröhling, 1999a,b). The presence of intercalated paleosols within a sand sheet sedimentological sequence indicates variable moisture conditions and/or variable sources of eolian sand during the LGM on the western Pampas. Similar loess–paleosol couplets, though more numerous (32) and spanning the past ca. 1.15 million years occur in northwestern Argentina (Tucúman Province) (Schellenberger and Veit, 2006). Unconformably capping the oldest eolian sand in the San Luis dune field are high-angle dune forest beds deposited in the past ca. 90 years. This 20th century interval of dune reactivation probably reflects landscape disturbance with overgrazing (Collado et al., 2002) exacerbated by drier conditions between 1870 and 1930 (Villalba et al., 1998; Compagnucci et al., 2002).

The Médanos Grandes dune field has a variety of surface forms, from kilometer to meter scale, reflecting complex eolian processes probably on 10^3 to 10^5 year time scales (Lancaster, 1999; Kocurek and Ewing, 2005). Thus, we consider the oldest OSL ages (ca. 4.2 ka), not dune field origination ages, but constraints on the subsequent reactivation of the Médanos Grandes dune field. The sedimentologic succession from sand sheet deposits to large-scale and opposing dune cross-beds dated to ca. 4.2 ka at the Zonda Site in the Médanos Grandes dune field and indicates rather recent migration of linear dunes, which are the dominate surface forms. This dune movement may be the culmination of regional aridity potentially initiated ca. 6 ka ago inferred from pollen records (D'Antoni, 1983; García et al., 1999; Mancini et al., 2005), discontinuous loess deposits (Sanabria and Argüello, 1999) and the decline in number of archaeologic sites in the southern Mendoza Province in western Argentina (Gil et al., 2005). Paleoecologic data from other areas of South and Central America document Mid-Holocene climate variability, demarcated by persistent aridity ca. 7 to 4 ka ago (e.g. Grosjean et al., 1997; Sandweiss et al., 1999; Iriarte et al., 2004). Linear dune formation in Médanos Grandes, western Argentina, at ca. 4.3–4.1 ka may reflect a landscape response to intensified drying, associated with rapid hemispheric environmental

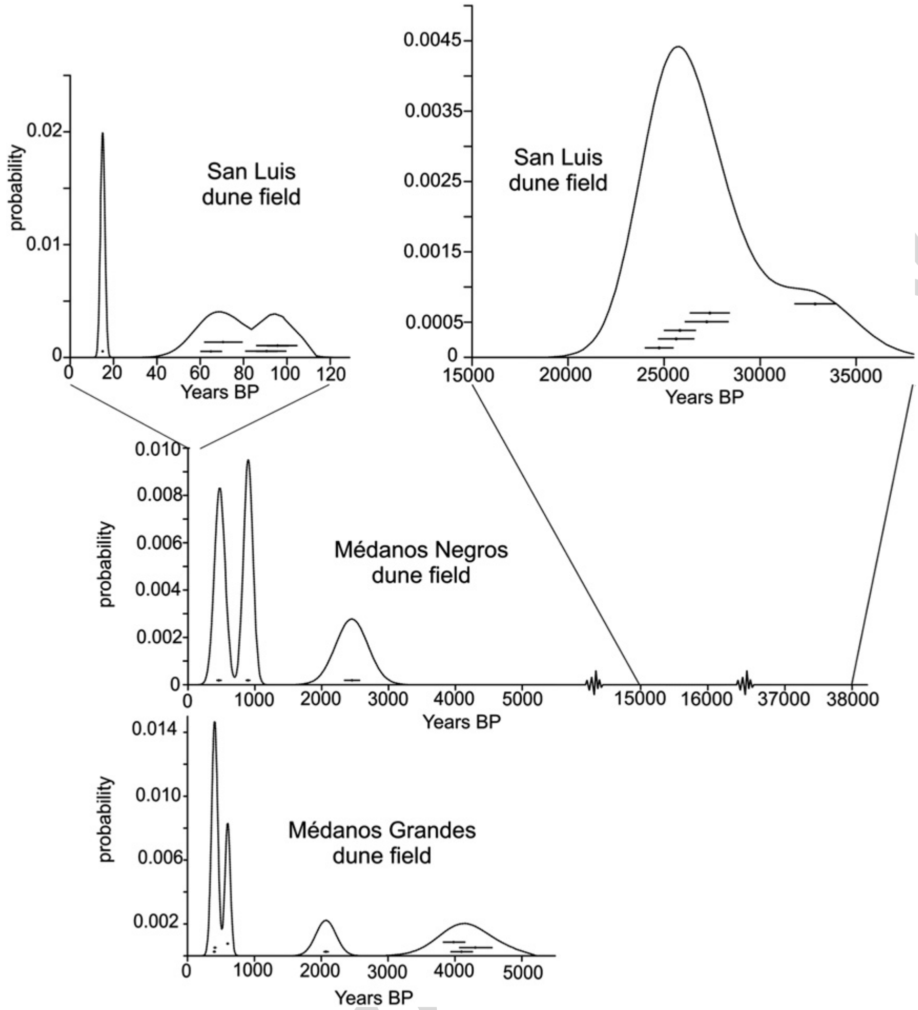

Fig. 14. Probability density distribution with one-sigma range for OSL ages on eolian sand deposits from Médanos Grande, Médanos Negros and San Luis dune fields, western Argentina. Horizontal bars indicate individual ages. For computational details, see Singhvi et al. (2001).

change, paced by changes in sea surface temperatures (Marchant and Hooghiemstra, 2004).

There is compelling evidence for repeated eolian sand deposition with dune migration in Médanos Grandes and Médanos Negros in the past ca. 3000 years. The Lizard Section exposes eolian sand over an alluvial fan sequence which shows the renewal of eolian deposition ca. 2100 years for the Médanos Grandes dune field, succeeded by discrete eolian deposition associated with dune migration ca. 600 to 400 years ago. OSL ages of ca. 2540, 475 and 900 years on low angle, cross-stratified sand from the Médanos Negros dune field indicate repeated late Holocene dune reactivation events, consistent with previously inferred timing (1–3 ka) of drying and dune movement (e.g. Iriondo and Kröhling, 1996; Kröhling, 1999a,b; Carignano, 1999) and discontinuous loess deposition (e.g. Sanabria and Argüello, 1999) in adjacent Córdoba Province. A possibly concurrent eolian depositional event is the initiation of eolian sand deposition over alluvial fan gravel at 2070 ± 150 years (UIC1719Bl) for Médanos Grande dune field and the latest movement of a dune ridge at 2540 ± 240 years (UIC1720Bl) for Médanos Negros dune field. At the Mascasín section in Médanos Negros the lower most massive eolian sand yield the optical age of 900 ± 70 years (UIC1605Bl). This section clearly exposes linear dunes that formed over salt-rich lake deposits. Thus, eolian deposition followed drying of this basin and signifies a shift to pronounced arid conditions at ca. 900 years ago. This period of aridity may be widespread with the initiation of eolian sand deposition in Córdoba Province (Kröhling and Iriondo, 1999) and loess deposition in Buenos Aires Province ca. 1200 to 900 years ago (Zárate and Blasi, 1991).

Another potentially concurrent eolian sand depositional event identified in Médanos Grandes and Médanos Negros dune fields occurred ca. 400–500 year ago and is consistent with previous observations on the formation of dunes and deflation basins and

the partial reactivation of dune forms in Córdoba Province (Cioccale, 1999); this shift may be coeval with inferred Little Ice Age aridity on the western Pampas (Kröhling and Iriondo, 1999; Iriondo, 1999). There is compelling evidence for a late Holocene period of dryness and subsequent aridity, though not chronologically well constrained, nor is it known if there were multiple decadal-to-century scale droughts that propagated dune movement.

9. Conclusions

This study of dune fields across western Argentina indicates a variable record of activity in the past 33 ka (Fig. 14). The San Luis paleo-dune field, currently the wettest locality, shows evidence for repeated activation during the LGM, ca. 33–20 ka, generally coincident with regional loess deposition (Iriondo and Kröhling, 1996; Kröhling, 1999a,b; Kemp et al., 2006; Zárate, 2003, and references therein). These dunes were locally reactivated in the past 100 years which is coeval with intensified agrarian use and drier climates in the late 19th and early 20th centuries (Villalba et al., 1998). The two driest and western-most dune fields, Médanos Grandes and Médanos Negros, show repeated reactivation in the past ca. 4 ka, with possibly concurrent eolian sand deposition ca. 2500–2100 and 400–600 years ago. This earlier period of aridity may be widespread with basins near the Brazilian coast at ca. 2200 years ago at the lowest water levels in past 5000 years (Sylvestre et al., 2005). The last episode of drying in Médanos Negros dune field commenced ca. 900 years ago with drying of an intermountain basin and subsequent migration of dune forms. The latest dune reactivation event in Médanos Grandes and Médanos Negros dune fields is at ca. 400–600 years ago and may be coincident with or slightly post-date the last neoglacial expansion in the adjacent Andes (Espizua, 2005). Uncertainty persists on spatial extent and duration of dune reactivation events, principally reflecting the scarcity of geochronometric constrained stratigraphic observations from the many stabilized dune fields in western Argentina.

Dune reactivation in western Argentina in past ca. 4500 years potentially reflects greater deficit in austral spring to summer precipitation than historically recognized (Compagnucci et al., 2002). Precipitation in western Argentina is associated with monsoon type circulation and concentrated (>70%) from October to March (Zhou and Lau, 1998; González et al., 2002). Drought conditions sufficient for at least partial reactivation of dune fields may reflect dynamic shifts in seasonal synoptic climatology, ultimately linked to changes in sea surface temperatures where the South Atlantic anticyclone is spawned (Zhou and Lau, 1998; Barros et al., 2002; González et al., 2002). Austral summer drying in western Argentina is associated with positive SSTs anomalies in the South Atlantic and a concomitant weakening and southern shift of South American Convergent Zone, with outflow from the moisture-laden Chaco Low Level Jet dispersed and shifted to the southeast. Thus, multi-year to-decadal scale droughts sufficient to induce dune reactivation reflect atmospheric “isolation” of moisture sources derived from the South Atlantic Ocean and the equatorial tropics.

Acknowledgments

This study was partially supported by a cooperative agreement between the University of Illinois and Department of Interior, National Park Service to forward a comparative analysis between North and South American dune fields. Additional funding was provided by Agencia Nacional de Promoción Científica y Técnica (PICT 07-10873) and CONICET (grant Res. 1269/04). Satellite images and meteorological data were supplied by CONAE and Servicio Meteorológico Nacional (Argentina), respectively. Support for field logistics was provided by University of Buenos Aires. We gratefully acknowledge the field assistance of P. Ciccioli, A. Quesada and H. Reijenstein and assistance with luminescence dating by J. Gomez, J. Pierson and C. Croughan. The comments of M. Zárate, J. Brigham-Grete and an anonymous reviewer are greatly appreciated.

References

Aitken, M.J., 1998. An Introduction to Optical Dating: The Dating of Quaternary Sediments by the Use of Photon-Stimulated Luminescence. Oxford University Press, NY.

Alcalde, J.A., Kulemeyer, J.J., 1999. The Holocene in the South-Eastern region of the Province Jujuy, North-West Argentina. Quaternary International 57/58, 113–116.

Barros, V.R., Silvestri, G.E., 2002. The relation between sea surface temperature at the subtropical south-central Pacific and precipitation in southeastern South America. Journal of Climate 15, 251–267.

Barros, V., Doyle, M., González, M., Camilloni, I., Bejarán, R., Caffera, R., 2002. Climate variability over subtropical South America and the South American monsoon: a review. Meteorologica 27, 31–55.

Birkeland, P., 1999. Soils and Geomorphology. Oxford University Press, New York.

Bøtter-Jensen, L., Bulur, E., Duller, G.A.T., Murray, A.S., 2000. Advances in luminescence instrument systems. Radiation Measurements 32, 523–528.

Carignano, C.A., 1999. Late Pleistocene to recent climate change is Córdoba Province, Argentina: geomorphological evidence. Quaternary International 57/8, 117–134.

Cioccale, M.A., 1999. Climatic fluctuations in the Central Region of Argentina in the last 1000 years. Quaternary International 62, 35–47.

Clapperton, C.M., 1993. Nature of environmental changes in South America at the Last Glacial Maximum. Palaeogeography, Palaeoclimatology, Palaeoecology 101, 189–208.

Collado, A.D., Chuvieco, E., Camarasa, A., 2002. Satellite remote sensing analysis to monitor desertification processes in the crop–rangeland boundary of Argentina. Journal of Arid Environments 52, 121–133.

Compagnucci, R.H., Agosta, E.A., Vargas, W.M., 2002. Climatic change and quasi-oscillations in central-west Argentina summer precipitation: main features and coherent behaviour with southern African region. Climate Dynamics 18 (5), 421–435.

D'Antoni, H., 1983. Pollen analysis of Gruta del Indio. Quaternary of South America and Antarctic Peninsula 1, 83–104.

Espizua, L.E., 2005. Holocene glacier chronology of Valenzuela Valley, Mendoza Andes, Argentina. The Holocene 15 (7), 1079–1085.

Fain, J., Soumana, S., Montret, M., Miallier, D., Pilleyre, T., Sanzelle, S., 1999. Luminescence and ESR dating-Beta-dose attenuation for various grain shapes calculated by a Monte-Carlo method. Quaternary Science Reviews 18, 231–234.

Forman, S.L., Oglesby, R., Webb, R., 2001. Patterns of Holocene dune activity on the great plains of North America: megadroughts and climate links. Global and Planetary Change 29, 1–29.

Forman, S.L., Marín, L., Pierson, J., Gómez, J., Miller, G.H., Webb, R.S., 2005. Aeolian sand depositional records from western Nebraska: landscape response to droughts in the past 1500 years. The Holocene 15 (7), 1–9.

Forman, S.L., Spaeth, M., Marín, L., Pierson, J., Gómez, J., Bunch, F., Valdez, A., 2006. Episodic Late Holocene dune movements on the sand-sheet area, Great Sand Dunes National Park and Preserve, San Luis Valley, Colorado, USA. Quaternary Research 66 (1), 97–108.

Fryberger, S.G., 1979. Dune forms and wind regime. In: McKee, E.D. (Ed.), A Study of Global Sand Seas. U.S. Geol. Survey Prof. Paper 1052, pp. 137–169.

García, A., Zárate, M., Paez, M.M., 1999. The Pleistocene–Holocene transition and human occupations in the Central Andes. Quaternary International 53/54, 43–52.

Gil, A., Zárate, M., Neme, G., 2005. Mid-Holocene paleoenvironments and the arqueological record of southern Mendoza, Argentina. Quaternary International 132, 81–94.

Goble, R.J., Mason, J.A., Loope, D.B., Swinehart, J.B., Loope, D.B., 2004. Optical and radiocarbon ages of stacked paleosols and dune sands in the Nebraska Sand Hills, USA. Quaternary Science Reviews 23, 1173–1182.

González, M., Barros, V., Doyle, M., 2002. Relation between the onset and end of the South American summer monsoon and rainfall in subtropical South America. Climate Research 21 (2), 141–155.

Grosjean, M., Nuñez, L., Cartajena, I., Messerli, B., 1997. Mid-Holocene climate and culture change in the Atacama Desert, northern Chile. Quaternary Research 48 (2), 239–246.

Havholm, K.G., Kocurek, G., 1988. A preliminary-study of the dynamics of a modern draa, algodones, Southeastern California, USA. Sedimentology 35 (4), 649–669.

Iriarte, J., Holst, I., Marozzi, O., Listopad, C., Alonso, E., Rinderknecht, A., Montana, J., 2004. Evidence for cultivar adoption and emerging complexity during the mid-Holocene in the La Plata basin. Nature 432 (7017), 614–617.

Iriondo, M., 1990. A late Holocene dry period in the Argentine plains. Quaternary of South America and Antarctic Peninsula 7, 198–218.

Iriondo, M., 1999. Climatic changes in the South American plains: records of a continent-scale oscillation. Quaternary International 57–58, 93–112.

Iriondo, M., García, N.O., 1993. Climatic variations in the Argentine plains during the last 18,000 years. Palaeogeography, Palaeoclimatology, Palaeoecology 101 (3–4), 209–220.

Iriondo, M., Kröhling, D., 1996. Los sedimentos eólicos del noreste de la llanura pampeana. XIII Congreso Geológico Argentino, Buenos Aires. Actas IV, pp. 27–48.

Jain, M., Botter-Jensen, L., Singhvi, A.K., 2003. Dose evaluation using multiple-aliquot quartz OSL: test of methods and a new protocol for improved accuracy and precision. Radiation Measurements 37, 67–80.

Jenny, B., Valero-Garcés, B.L., Villa-Martinez, R., Urrutia, R., Geyh, M., Veit, H., 2002. Early to mid-Holocene aridity in central Chile and the southern Westerlies: the Laguna Aculeo record (34° S). Quaternary Research 58 (2), 160–170.

Kemp, R.A., Toms, P.S., King, M., Kröhling, D.M., 2004a. The pedosedimentary evolution and chronology of Tortugas, a Late Quaternary type-site of the northern Pampa, Argentina. Quaternary International 114 (1), 101–112.

Kemp, R.A., King, M., Toms, P., Derbyshire, E., Sayago, J.M., Collantes, M.M., 2004b. Pedosedimentary development of part of a Late Quaternary loess–palaeosol sequence in Northwest Argentina. Journal of Quaternary Science 19, 567–576.

Kemp, R.A., Zárate, M., Toms, P., King, M., Sanabria, J., Argüello, G., 2006. Late Quaternary paleosols, stratigraphy and landscape evolution in the Northern Pampa, Argentina. Quaternary Research 66 (1), 119–132.

Kocurek, G., Ewing, R., 2005. Aeolian dune field self-organization—implications for the formation of simple versus complex dune-field patterns. Geomorphology 72, 94–105.

Kocurek, G., Lancaster, N., 1999. Aeolian system sediment state: theory and Mojave Desert Kelso dune field example. Sedimentology 46 (3), 505–515.

Kröhling, D.M., 1999a. Sedimentological maps of the typical loessic units in North Pampa, Argentina. Quaternary International 62 (1), 49–55.

Krohling, D.M., 1999b. Upper Quaternary geology of the lower Carcarana Basin, North Pampa, Argentina. Quaternary International 57–8, 135–148.

Kröhling, D.M., Iriondo, M., 1999. Upper Quaternary palaeoclimates of the Mar Chiquita area, North Pampa, Argentina. Quaternary International 57–8, 149–163.

Lancaster, N., 1999. Geomorphology of desert sand seas. In: Goudie, A.S., Livingstone, I., Stokes, S. (Eds.), Aeolian Environments, Sediments and Landforms. Wiley, New York, pp. 49–69.

Mancini, M.V., Paez, M.M., Prieto, A.R., Stutz, S., Tonello, M., Vilanova, I., 2005. Mid-Holocene climatic variability reconstruction from pollen records (32°–52°S, Argentina). Quaternary International 132 (1), 47–59.

Marchant, R., Hooghiemstra, H., 2004. Rapid environmental change in African and South American tropics around 4000 years before present: a review. Earth-Science Reviews 66 (3–4), 217–260.

Markgraf, V., 1989. Paleoclimates in Central and South-America since 18,000 BP Based on Pollen, Lake-Level Records. Quaternary Science Reviews 8 (1), 1–24.

Martin, L., Fournier, M., Mourguiart, P., Sifeddine, A., Turcq, B., Absy, M.L., Flexor, J.M., 1993. Southern Oscillation Signal in South-American Paleoclimatic Data of the Last 7000 Years. Quaternary Research 39 (3), 338–346.

Mejdahl, V., Christiansen, H.H., 1994. Procedures used for luminescence dating of sediments. Boreas 13, 403–406.

Muhs, D.R., Zárate, M., 2001. Late Quaternary Eolian records of the Americas and their paleoclimatic significance. In: Markgraf, V.

(Ed.), Interhemispheric Climate Linkages. Academic Press, New York, pp. 183–216.

Murray, A.S., Wintle, A.G., 2000. Luminescence dating of quartz using an improved single-aliquot regenerative-dose protocol. Radiation Measurements 32, 57–73.

Murray, A.S., Wintle, A.G., 2003. The single aliquot regenerative dose protocol: potential for improvements in reliability. Radiation Measurements 37, 377–381.

Olley, J.M., Pietsch, T., Roberts, R.G., 2004. Optical dating of Holocene sediments from a variety of geomorphic settings using single grains of quartz. Geomorphology 60 (3–4), 337–358.

Piovano, E.L., Ariztegui, D., Bernasconi, S.M., McKenzie, J.A., 2004. Stable isotopic record of hydrological changes in subtropical Laguna Mar Chiquita (Argentina) over the last 230 years. The Holocene 14 (4), 525–535.

Prescott, J.R., Hutton, J.T., 1994. Cosmic ray contributions to dose rates for luminescence and ESR dating: large depths and long-term time variations. Radiation Measurements 23, 497–500.

Prieto, A.R., 1996. Late Quaternary vegetational and climatic changes in the Pampa Grassland of Argentina. Quaternary Research 45 (1), 73–88.

Richardson, C.A., 1994. Effects of bleaching on the Sensitivity to dose of the infrared-stimulated luminescence of potassium-rich feldspars from Ynyslas, Wales. Radiation Measurements 23 (2–3), 587–591.

Sanabria, J., Argüello, G., 1999. La edad de los materiales parentales loéssicos de los suelos y desarrollo del perfil, en un sector de la plataforma basculada, Córdoba, Argentina. XVI Congreso Latinoamericano de la Ciencia del Suelo, Temuco, Chile, Resúmenes, pp. 210–214.

Sandweiss, D.H., Maasch, K.A., Anderson, D.G., 1999. Climate and culture—transitions in the mid-Holocene. Science 283 (5401), 499–500.

Saulo, A.C., Nicolini, M., Chou, S.C., 2000. Model characterization of the South American low-level flow during the 1997–1998 spring–summer season. Climate Dynamics 16 (10–11), 867–881.

Sayago, J.M., Collantes, M.M., Karlson, A., Sanabria, J., 2001. Genesis and distribution of the Late Pleistocene and Holocene loess of Argentina: a regional approximation. Quaternary International 76–77, 247–257.

Schellenberger, A., Veit, H., 2006. Pedostratigraphy and pedological and geochemical characterization of Las Carreras loess–paleosol sequence, Valle de Tafí, NW-Argentina. Quaternary Science Reviews 25, 811–831.

Servicio Meteorológico Nacional, 1958a. Estadísticas Climatológicas 1901–1950. Buenos Aires.

Servicio Meteorológico Nacional, 1958b. Estadísticas Climatológicas 1941–1950. Buenos Aires.

Servicio Meteorológico Nacional, 1969. Estadísticas Climatológicas 1951–1960. Buenos Aires.

Servicio Meteorológico Nacional, 1975. Estadísticas Climatológicas 1961–1970. Buenos Aires.

Servicio Meteorológico Nacional, 1986. Estadísticas Climatológicas 1971–1980. Buenos Aires.

Servicio Meteorológico Nacional, 1994. Estadísticas Climatológicas 1981–1990. Buenos Aires.

Singhvi, A.K., Sharma, Y.P., Agrawal, D.P., 1982. Thermoluminescence dating of dune sands in Rajasthan, India. Nature 295, 313–315.

Singhvi, A.K., Bluszcz, A., Bateman, M.D., Rao, M.S., 2001. Luminescence dating of loess–palaeosol sequences and coversands: methodological aspects and palaeoclimatic implications. Earth-Science Reviews 54 (1–3), 193–211.

Sylvestre, F., Sifeddine, A., Turcq, B., Gil, I., Albuquerque, M., Lallier-Verges, A.L.S., Abrao, E., 2005. Hydrological changes related to the variability of tropical South American climate from the Cabo Frio lagoonal system (Brazil) during the last 5000 years. The Holocene 15 (4), 625–630.

Tripaldi, A., 2002a. Sedimentología y evolución del campo de dunas de Médanos Grandes (provincia de San Juan, Argentina). Revista de la Asociación Argentina de Sedimentología 9, 65–82.

Tripaldi, A. 2002b. Análisis sedimentológico de depósitos eólicos de valles intermontanos, su aplicación al estudio de secuencias terciarias del noroeste argentino. PhD Thesis, Universidad de Buenos Aires, Argentina.

Tripaldi, A., Limarino, C.O., 2004. Hierarchic Classification and Mapping of Modern Eolian fields of Northwestern Argentina. 32nd International Geological Congress, Florence, Italy, Abs., vol. 1, p. 256.

Valero-Garcés, B., Arenas, C., Delgado-Huertas, A., 2001. Depositional environments of Quaternary lacustrine travertines and stromatolites from high-altitude Andean lakes, northwestern Argentina. Canadian Journal of Earth Sciences 38 (8), 1263–1283.

Villagrán, C., Varela, J., 1990. Palynological evidence for increased aridity on the central Chilean coast during the Holocene. Quaternary Research 34 (2), 198–207.

Villalba, R., 1994. Tree-ring and glacial evidence for the medieval warm epoch and the little Ice-Age in Southern South-America. Climatic Change 26 (2–3), 183–197.

Villalba, R., Grau, H.R., Boninsegna, J.A., Jacoby, G.C., Ripalta, A., 1998. Tree-ring evidence for long-term precipitation changes in subtropical South America. International Journal of Climatology 18 (13), 1463–1478.

Wang, M.Y., Paegle, J., 1996. Impact of analysis uncertainty upon regional atmospheric moisture flux. Journal of Geophysical Research-Atmospheres 101 (D3), 7291–7303.

Zárate, M., 2003. Loess of southern South America. Quaternary Science Reviews 22, 1987–2006.

Zárate, M., Blasi, A., 1991. Late Pleistocene and Holocene deposits of the southeastern Buenos Aires Province, Argentina. Geojournal 24 (2), 211–220.

Zárate, M., Blasi, A., 1993. Late Pleistocene and Holocene deposits of the southeastern Buenos Aires Province: a preliminary model. Quaternary International 17, 15–20.

Zhou, J.Y., Lau, K.M., 1998. Does a monsoon climate exist over South America? Journal of Climate 11 (5), 1020–1040.